The DOI for this manuscript is doi: 10.1175/BAMS-D-17-0212.1

The global N_2O Model Intercomparison Project (NMIP): Objectives, Simulation Protocol and Expected Products

Hanqin Tian[1,2], Jia Yang[1,2], Chaoqun Lu[1,3], Rongting Xu[1], Josep G Canadell[4], Robert Jackson[5], Almut Arneth[6], Jinfeng Chang[7], Guangsheng Chen[1,2], Philippe Ciais[7], Stefan Gerber[8], Akihiko Ito[9], Yuanyuan Huang[7, 8], Fortunat Joos[10,11], Sebastian Lienert[10,11], Palmira Messina[7], Stefan Olin[12], Shufen Pan[1,2], Changhui Peng[13, 14], Eri Saikawa[15], Rona L. Thompson[16], Nicolas Vuichard[7], Wilfried Winiwarter[17, 18], Sönke Zaehle[19], Bowen Zhang[1], Kerou Zhang[14], Qiuan.Zhu[14]

[1] International Center for Climate and Global Change Research, School of Forestry and Wildlife Sciences, Auburn University, Auburn, AL 36849, USA
[2] Research Center for Eco-Environmental Sciences, Chinese Academy of Sciences, State Key Laboratory of Urban and Regional Ecology, Beijing 100085, China
[3] Department of Ecology, Evolution, and Organismal Biology, Iowa State University, IA 50011, USA
[4] Global Carbon Project, CSIRO Oceans and Atmosphere, Canberra, Australia
[5] Department of Earth System Science, Woods Institute for the Environment, and Precourt Institute for Energy, Stanford University, Stanford, CA 94305-2210
[6] Karlsruhe Institute of Technology, Institute of Meteorology and Climate Research/Atmospheric Environmental Research, 82467 Garmisch-Partenkirchen, Germany
[7] Laboratoire des Sciences du Climat et de l'Environnement, LSCE, 91191 Gif sur Yvette, France
[8] University of Florida, IFAS, Soil and Water Sciences Department, Gainesville, FL, 32611-0510, USA
[9] Center for Global Environmental Research, National Institute for Environmental Studies, Tsukuba, 3058506, Japan
[10] Climate and Environmental Physics, Physics Institute, University of Bern, Bern, Switzerland
[11] Oeschger Centre for Climate Change Research, University of Bern, Bern, Switzerland
[12] Department of Physical Geography and Ecosystem Science, Lund University, S-223 62 Lund, Sweden
[13] Department of Biology Sciences, University of Quebec at Montreal (UQAM), Montréal (Québec), H3C 3P8, Canada
[14] Center for Ecological Forecasting and Global Change, College of Forestry, Northwest A&F University, Yangling, Shaanxi 712100, China
[15] Department of Environmental Sciences, Emory University, Atlanta, GA, USA
[16] Norsk Institutt for Luftforskning - NILU, Kjeller, Norway
[17] Air Quality and Greenhouse Gases (AIR), International Institute for Applied Systems Analysis, Schlossplatz 1A-2361 Laxenburg, Austria
[18] The Institute of Environmental Engineering, University of Zielona Gora, Licealna 9, 65-417 Zielona Gora, Poland
[19] Max Planck Institut für Biogeochemie, P.O. Box 600164, Hans-Knöll-Str. 10, 07745 Jena, Germany

Corresponding author: Hanqin Tian (tianhan@auburn.edu)

Bulletin of the American Meteorological Society (BAMS)
Revised Manuscript (12/26/2017)

Abstract

Nitrous oxide (N_2O) is an important greenhouse gas (GHG) and also an ozone-depleting substance that has both natural and anthropogenic sources. Large uncertainty remains on the magnitude and spatiotemporal patterns of N_2O fluxes and the key drivers of N_2O production in the terrestrial biosphere. Some terrestrial biosphere models have been evolved to account for nitrogen processes and show the capability to simulate N_2O emissions from land ecosystems at the global scale, but large discrepancies exist among their estimates primarily due to inconsistent input data sets, simulation protocol, and model structure and parameterization schemes. Based on the consistent model input data and simulation protocol, the global N_2O Model Inter-Comparison Project (NMIP) was initialized with ten state-of-the-art terrestrial biosphere models with N cycling included. Specific objectives of NMIP are to: 1) Unravel the major N cycling processes controlling N_2O fluxes in each model and identify the uncertainty sources from model structure, input data and parameters; 2) Quantify the magnitude, spatial and temporal patterns of global and regional N_2O fluxes from the pre-industrial period (1860) to present, and attribute the relative contributions of multiple environmental factors to N_2O dynamics; and 3) Provide a bench-marking estimate of N_2O fluxes through synthesizing the multi-model simulation results and existing estimates from ground-based observations, inventories, and statistical and empirical extrapolations. This study provides detailed descriptions for the NMIP protocol, input data, model structure and key parameters, along with preliminary simulation results. The global and regional N_2O estimation derived from the NMIP is a key component of the Global N_2O Budget activity jointly led by the Global Carbon Project (GCP) and the International Nitrogen Initiative (INI).

Capsules

The N_2O Model Inter-Comparison Project (NMIP) aims at understanding and quantifying the budgets of global and regional terrestrial N_2O fluxes, environmental controls and uncertainties associated with input data, model structure and parameters.

1. Introduction

Nitrous oxide (N_2O) is an important greenhouse gas and the time-integrated radiative forcing resulting from a mass unit of N_2O is 298 times larger than that from carbon dioxide (CO_2) emissions for a 100-year time horizon (Ciais et al., 2013; Myhre et al., 2013). Multiple lines of evidence indicate that human activities (e.g., industrial N_2 fixation by the Haber-Bosch process or by combustion, and manure N application) play an increasingly significant role in the perturbation of the global N cycle (Galloway et al., 2008; Gruber et al., 2008; Fowler et al., 2015), which has led to an increase in atmospheric N_2O concentration by ~21%, from 271 ppb at pre-industrial level to 329 ppb in 2015 (MacFarling et al., 2006; Prather et al., 2012, 2015; Thompson et al., 2014; https://www.esrl.noaa.gov/). The anthropogenic N_2O emissions are estimated to have increased from 0.7 Tg N yr^{-1} in 1860 to 6.9 Tg N yr^{-1} in 2006, ~60% of which was ascribed to agricultural activities (Ciais et al., 2013, Davidson and Kanter, 2014). The increased N_2O emissions have significantly contributed to climate warming. During the 2000s, the warming effect of N_2O emissions from the terrestrial biosphere counteracted more than half of the cooling effect of the global land CO_2 sink (Tian et al., 2016), and anthropogenic N_2O emissions are projected to lead to further global warming during the 21st century and beyond (Stocker et al., 2013).

In terrestrial ecosystems, N_2O is mainly produced in soils via nitrification and denitrification processes (Smith and Arah, 1990; Wrage et al., 2001; Schmidt et al., 2004). All these processes are regulated by microbial activities under various soil micro-environments such as soil temperature, moisture and aeration, clay content, pH, and C and N availability (Firestone and Davidson, 1989; Goldberg and Gebauer, 2009; Butterbach-Bahl et al., 2013; Brotto et al., 2015; Rowlings et al., 2015). In addition, N_2O emissions from terrestrial ecosystems can be

112 regulated by both natural disturbances and human management such as synthetic N fertilizer,
113 manure N application, irrigation, tillage, and the choice of crop varieties (Rice and Smith, 1982;
114 Cai et al., 1997; Ding et al., 2010). However, our understanding of the mechanisms responsible
115 for terrestrial N_2O emissions is still limited, which contributes to large uncertainties in estimating
116 both preindustrial and contemporary N_2O emissions. For example, estimates of global terrestrial
117 N_2O emissions from natural sources vary by up to a factor of three and range between 3.3 and
118 9.0 Tg N yr^{-1} (Ciais et al. 2013). Human-induced biogenic N_2O emissions from the land
119 biosphere have not yet been investigated well (Tian et al. 2016). Therefore, a major international
120 and multidisciplinary effort is required to assess information from different research disciplines
121 and approaches in order to constrain current knowledge on the N_2O budget and drivers, and to
122 identify research gaps.

123 Process-based modeling is an essential tool in assessing and predicting the terrestrial N
124 cycle and N_2O fluxes in response to multi-factor global changes. Several process-based models
125 have been used to estimate N_2O emissions from natural and agricultural soils at various
126 spatiotemporal scales. The conceptual model of "hole-in-pipe" (Firestone and Davidson, 1989)
127 was first incorporated in the Carnegie-Ames-Stanford-Approach (CASA) Biosphere model
128 (Potter et al., 1993) to estimate N trace gas emissions at the global scale (Potter et al., 1996). The
129 daily version of the CENTURY model (DAYCENT) was linked to atmospheric models to better
130 estimate trace gas fluxes from different ecosystems (Parton et al., 1998). The DeNitrification-
131 DeComposition model (DNDC; Li et al., 1992) was developed to study the impacts of various
132 agricultural practices on N_2O emissions. In the Dynamic Land Ecosystem Model (DLEM), Tian
133 et al. (2011, 2015) considered the biotic and abiotic processes (e.g., plant N uptake and N
134 leaching loss) that regulate N_2O fluxes in natural and managed soils. In recent years, multiple C-

N coupled models, such as DyN-LPJ (Xu-Ri and Prentice, 2008), O-CN (Zaehle and Friend, 2010, 2011), Land Surface Processes and exchanges model of the University of Bern (LPX-Bern 1.0; Stocker et al., 2013), CLMCN-N_2O (Saikawa et al., 2014), and LM3V-N (Huang and Gerber, 2015) were developed by integrating a prognostic N cycle into different land surface models and simulate N_2O emissions from land ecosystems. Unsurprisingly, these models generated divergent estimates of global terrestrial N_2O budgets and spatiotemporal patterns mainly due to differences in model input datasets, model structure, and parameterization schemes. What are the major contributing factors responsible for the changing patterns of terrestrial N_2O emissions? How can we narrow down the model-estimated bias or uncertainties? What are the knowledge gaps in fully accounting for the N_2O processes? Here, we attempt to answer these questions through the establishment and designing of the global N_2O Model Inter-comparison Project (NMIP).

During the past two decades, carbon-related Model Intercomparison Projects (MIPs) have been established to evaluate model uncertainties in simulating the terrestrial carbon dynamics. For example, the Vegetation-Ecosystem Modeling and Analysis Project (VEMAP) was a pioneer MIP activity, driven by a common model input database and was established to provide multi-model ensemble estimates of carbon fluxes and storage in response to changing climate and atmospheric CO_2 (Melillo et al., 1995; Schimel et al., 2000). More recently, a number of CO_2-oriented MIPs and synthesis activities were implemented, such as the North American Carbon Program site and regional synthesis (NACP; Schwalm et al., 2010; Richardson et al., 2011; Schaefer et al., 2012) and its extended Multi-Scale Synthesis and Terrestrial Model Intercomparison Project (MsTMIP; Huntzinger et al., 2013; Wei et al., 2014), the TRENDY Project (Le Quéré et al., 2016; Sitch et al., 2015), the Inter-Sectoral Impact Model Intercomparison Project (ISI-MIP) (Warszawski et al., 2014; Ito et al., 2016), and the Multi

158 Model-data Synthesis of Terrestrial Carbon Cycles in Asia (Asia-MIP; Ichii et al., 2013). These
159 MIPs enhanced our understanding of model uncertainties and provided insight into future
160 directions of model improvement.

161 Following the CO_2-related MIPs, global methane (CH_4) MIPs and synthesis activities
162 were implemented in recent years, for example, the Wetland and Wetland CH_4 Intercomparison
163 of Models Project (WETCHIMP; Melton et al., 2013; Wania et al., 2013) and GCP global CH_4
164 budget synthesis (Saunois et al., 2016; Poulter et al. 2017). Although terrestrial biogenic N_2O
165 emissions significantly contribute to climate warming, the model development for simulating N
166 cycle and N_2O fluxes remains far behind the CO_2- and CH_4-related activities. The relatively
167 sparse and short-term observations limited our understanding of N cycling in terrestrial
168 ecosystems. Comparing with CO_2 and CH_4, smaller N_2O concentration gradients in the
169 atmosphere and the varying magnitudes of soil N_2O emissions across observation sites and
170 periods makes it more difficult to quantify the N_2O budget at a large scale. Another important
171 uncertainty comes from the differences in model representation and parameterization schemes of
172 N processes, and the influence of biophysical and environmental factors on N_2O dynamics
173 (Appendix A). Similar to the purposes of the CO_2- and CH_4-related MIPs, there is a need to
174 initialize a MIP for the N models to assess the global N_2O budget. Under the umbrella of the
175 Global Carbon Project (GCP) and the International Nitrogen Initiative (INI), we initiated the
176 NMIP to investigate the uncertainty sources in N_2O estimates and provide multi-model N_2O
177 emissions estimates from natural and agricultural soils. This paper describes the detailed NMIP
178 protocol, input data, model structure, and some preliminary simulation results.
179

180 **2. The NMIP framework, objectives and tasks**

Motivated by large uncertainties and increasing data availability, the NMIP is developed to establish a research network for providing a multi-model ensemble estimate on the global/regional N_2O budgets and to identify major uncertainties associated with model structure, parameters and input data (Figure 1). This project was first proposed at the Regional Carbon Cycle Assessment and Processes (RECCAP) workshop "4th International workshop on Asian Greenhouse Gases", in JAMSTEC, Yokohama, Japan, April 8-10, 2014. The NMIP was launched at a side meeting during the 2015 American Geophysical Union fall meeting and began to work in the fall of 2016.

Specific objectives of NMIP are: 1) Unravel the major N cycling processes controlling N_2O fluxes in each model and identify the uncertainty sources from modeling structure, input data and parameters; 2) Quantify the magnitude, spatial and temporal patterns of global and regional N_2O fluxes during 1860–2015, and attribute the relative contributions of multiple environmental factors to N_2O dynamics; and 3) Provide a bench-mark estimate of global/regional N_2O fluxes through synthesizing the multi-model simulation results and existing estimates from ground-based observations, inventories, and statistical/empirical extrapolations. To achieve these objectives, the NMIP group members have collectively developed a model simulation protocol as outlined in Figure 1.

There are five key tasks or progressing stages in the protocol: 1) Development and delivery of spatiotemporal model driving forces; 2) Individual model calibration and evaluation; 3) Model simulations and delivery of results; 4) Quality control and analysis of model results; 5) Synthesis and uncertainty analysis.

3. Key model input datasets

To minimize the uncertainty that results from input datasets, the NMIP provided consistent model driving datasets for all modeling groups. The datasets include potential vegetation, climate, atmospheric CO_2 concentration, atmospheric N deposition, synthetic N fertilizer applications in cropland and pasture, manure N production and applications in cropland and pasture, and historical distribution of cropland at a spatial resolution of 0.5° by 0.5° latitude/longitude (Table 1). Half-degree resolution is appropriate for studies at a global scale, considering that most of model input data are available and many previous MIPs at a global scale were conducted at this resolution. Here we briefly describe these input data sets and their sources.

1) Climate: CRU-NCEP climate version 7 is a fusion of the CRU and NCEP/NCAR reanalysis climate datasets between 1901 and 2015, which was reconstructed by the Laboratoire des Sciences du Climat et l'Environnement, Paris, France (https://vesg.ipsl.upmc.fr). Major climate variables include longwave and shortwave radiation, air pressure, humidity, temperature, precipitation, and wind speed at 6-hourly temporal resolution. Monthly magnitude of climate variables in CRU-NCEP dataset was forced to be consistent with the observational-based CRU datasets.

2) Atmospheric CO_2: Monthly atmospheric CO_2 concentration from 1860 to 2015 was obtained from NOAA GLOBALVIEW-CO_2 dataset derived from atmospheric and ice core measurements (https://www.esrl.noaa.gov).

3) Vegetation: Potential vegetation map was acquired from the Synergetic Land Cover Product (SYNMAP, ftp://ftp.bgc-jena.mpg.de/pub/outgoing/mjung/SYNMAP/), which merged multiple satellite-global land cover maps into a desired classification approach (Jung et al., 2006). Each 0.5° grid cell includes the area fractions for a maximum of 47 land cover types. Vegetation

in SYNMAP is classified according to its life form, leaf type, and leaf longevity. Barren ground, permanent snow and ice are also included in this dataset. Based on this SYNMAP dataset, participating model groups could create vegetated land fraction and reorganize the vegetation types to generate the corresponding plant functional type and fractions for their models. Annual cropland area from 1860 to 2015 was acquired from the HYDE 3.2 datasets (ftp://ftp.pbl.nl/hyde/), which reconstructed time-dependent land use by historical population and allocation algorithms with weighting maps (Klein Goldewijk et al., 2016). This dataset shows that global cropland area increased from 5.9 million km^2 in the year of 1850 to 15.2 million km^2 in the year of 2015.

4) Atmospheric N deposition onto land surface: The monthly atmospheric N deposition (NHx-N and NOy-N) during 1860 - 2014 were from the IGAC/SPARC Chemistry-Climate Model Initiative (CCMI) N deposition fields. CCMI models explicitly considered N emissions from natural biogenic sources, lightning, anthropogenic and biofuel sources, and biomass burning (Eyring et al., 2013). The transport of N gases has also been simulated by the chemical transport module in CCMI models. This data was recommended by the Coupled Model Intercomparison Project (CMIP) and used as the official products for CMIP6 models that lack interactive chemistry components (https://blogs.reading.ac.uk/ccmi/forcing-databases-in-support-of-cmip6/).

5) N fertilizer application: Spatially-explicit synthetic N fertilizer use data was specifically developed in this project. We reconstructed the annual synthetic/mineral N fertilizer dataset from 1960 to 2014 for the global cropland, matched with HYDE 3.2 cropland distribution (Lu and Tian, 2017; https://doi.pangaea.de/10.1594/PANGAEA.863323). Data on national-level crop-specific fertilizer use amount was collected from the International Fertilizer Industry

Association (IFA) and FAO. This N fertilizer dataset shows that the global total N fertilizer amount increased from 11 Tg N yr^{-1} in 1960 to 112 Tg N yr^{-1} in 2013, and N fertilizer use rate per unit cropland area increased by about 8 times in this period. N fertilizer application rate before 1960 was linearly reduced to the zero in the 1900s.

6) Manure N production and application: Gridded annual manure N production in the period of 1860-2014 was developed by integrating the Global Livestock Impact Mapping System (GLIMS), the country-level livestock population from FAO, and N excretion rates of different livestock categories according to IPCC 2006-Tier I and (Zhang et al., 2017, https://doi.org/10.1594/PANGAEA.871980). This annual dataset shows that manure N production increased by more than 6 times from 21 Tg N yr^{-1} in 1860 to 131 Tg N yr^{-1} in 2014, and application rate of manure N to cropland is less than 20% of the total production. In this project, we only consider the manure N application in cropland area. Manure N production and application rates in 2015 was assumed to be same as that in 2014.

All the input datasets were delivered to the modeling groups in netCDF format. To fit with individual modeling requirements for input datasets, the modeling groups could either use a subset of these data sets or add some additional data sets. For example, the participating model DLEM used all these environmental factors as inputs, while the model O-CN did not use manure N as an input (See Table 3 for model input requirements in each model). Figure 2 illustrates the inter-annual variations of the major input datasets at the global level during different available time periods. Figure 3 shows the spatial patterns of atmospheric N deposition, N fertilizer use, and manure N production in 1860, 1900, 1950, and 2014.

4. Model result benchmarking and evaluation

Except for bottom-up model simulations, the NMIP also plans to synthesize multiple sources of terrestrial soil N_2O emission data to provide a benchmark for evaluating model estimates. Four types of data will be collected or developed to serve as a potential benchmark: 1) Site-level N cycling processes and N_2O emission measurements through chamber or eddy-flux tower across biomes; 2) N_2O flux measurement data from national-based or global-based measurement network (e.g., Long Term Ecological Research Network, Long Term Agroecosystem Research Network, Greenhouse gas Reduction through Agriculture Carbon Enhancement network, http://www.n2o.net.au, etc.) ; 3) Other spatialized datasets, including statistical extrapolation (e.g., Xu et al. 2008; Kurokawa et al., 2013; Zhuang et al., 2012); 4) N_2O fluxes from other than terrestrial ecosystem sources to allow for a global budget (industrial, combustion, waste water & water bodies, marine and oceanic sources) (e.g., Battaglia and Joos, in press; Davidson and Kanter, 2014; Galloway et al., 2004; Fowler et al., 2013; Winiwarter et al., 2017); and 5) atmospheric inversions (e.g., Saikawa et al., 2014; Thompson et al., 2014) in conjunction with atmospheric N_2O measurements from tall towers. We also call for more observation-derived studies to provide regional and global N_2O emission estimates through advanced computational techniques, such as machine learning, Multi-Tree Ensemble (MTE), and remote sensing products. We anticipate that through multiple constraints, process-based modeling approach can be more effective and reliable in estimating magnitude, spatial and temporal patterns of terrestrial N_2O emissions, and quantifying relative contributions of environmental drivers to N_2O dynamics.

5. Major characteristics of participating models

The N cycle in the earth system involves complex biogeochemical processes, in which N is transformed into various chemical forms, and circulates among the atmosphere, terrestrial and aquatic ecosystems. Important terrestrial processes in the N cycle include biological N fixation (BNF), mineralization (conversion of organic N to inorganic N during the processes of organic matter decomposition), immobilization (transformation of soil inorganic N to organic N), ammonification (conversion of organic to ammonium N), volatilization (transformation of soil ammonium N to ammonia gas), nitrification (transformation of ammonium N to nitrate and nitrite N), denitrification (the process of nitrate reduction by microbial activities), plant uptake from soil, resorption by living plant organs, adsorption and desorption by soil mineral particles, and N leaching from soil to aquatic systems. The modeled N processes include N transformation between organic and inorganic forms and movements among atmosphere, vegetation, soil, and riverine systems. Although N processes are tightly coupled with carbon processes in soil and vegetation, the greater variability in N processes compared to C processes make it more difficult to simulate N cycling. At current stage, the NMIP has included ten ecosystem models with explicit terrestrial N cycling processes (Table 2; Figure 1). Nine models (DLEM, LM3V-N, ORCHIDEE, ORCHIDEE-CNP, O-CN, LPJ-GUESS, LPX-Bern, TRIPLEX-GHG and VISIT) are capable of simulating N_2O emissions from both natural and agriculture ecosystems, while one model (CLM-CN) only simulates N_2O emissions from natural vegetation. The biophysical processes (such as, canopy structure, albedo and evapotranspiration), biogeochemical processes (such as decomposition and denitrification), and N input for cropland are significantly different from those for natural vegetation. For example, temperature in cropland was found to be lower than that in natural forest due to the higher albedo and evapotranspiration (Bonan, 2000). These differences could lead to different magnitude and timing of N_2O emissions from cropland.

Therefore, biophysical characteristics and management practices in cropland, such as crop cultivation, fertilizer uses, irrigation and harvesting, are required to be explicitly represented by the models with crop module.

In order to assess the uncertainty from model structure, each participating model was asked to complete a detailed survey specifying the modeling mechanisms in exogenous N inputs (e.g., N deposition, synthetic N fertilizer and manure N application, and BNF) and N transformation processes. The summarized survey results are shown in Table 3. In general, N_2O emissions from soil are regulated at two levels, which are the rates of nitrification and denitrification in the soil and soil physical factors regulating the ratio of N_2O to other nitrous gases (Davidson et al., 2000).

For N input to land ecosystems, all ten models considered the atmospheric N deposition and biological fixation, nine models with a crop N_2O module included N fertilizer use, but only six models considered manure as N input. For vegetation processes, all models included dynamic algorithms in simulating N allocation to different living tissues and vegetation N turnover, and simulated plant N uptake using the "Demand and Supply-driven" approach. For soil N processes, all ten models simulated N leaching according to water runoff rate; however, the models differ in representing nitrification and denitrification processes and the impacts of soil chemical and physical factors. The differences in simulating nitrification and denitrification processes are one of the major uncertainties in estimating N_2O emissions. Algorithms associated with N_2O emissions in each participating model are briefly described in Appendix A.

6. The NMIP model simulation methods and experimental designs

6.1 Model initialization

The model simulations were divided into two stages: (1) spin-up and (2) transient runs (Figure 4). During the spin-up run, models were driven by the repeated climate data from 1901 - 1920 and by other driving forces in 1860, i.e., atmospheric CO_2 concentration, N deposition, N fertilizer use, manure N application, and land cover and land use change (LCLU). The N fertilizer use was assumed to be zero in 1860. Each model group could determine the spin-up running years according to model's specific requirement. For example, the DLEM assumed that model reaches the equilibrium status when the differences of grid-level carbon, N, and water stocks were less than 0.5 g C m^{-2}, 0.5 g N m^{-2}, and 0.5 mm in two consecutive 50 years. When these thresholds were met, the spin-up run stopped and model reached an equilibrium state.

6.2 Model simulation experiments

During the transient run, seven experiments were designed to simulate global terrestrial N_2O emissions. All the model experiments started with the equilibrium carbon, water and N status in 1860, which is obtained from the spin-up run, and transiently ran through the period during 1860-2015 (Figure 4). For the period of 1860-1900 when CRU/NCEP climate data is not available, the 20-year average climate data between 1901 and 1920 were used. In the NMIP, we applied the progressively reducing factor experimental scheme (i.e., first experiment includes all factors and then reduce one factor each time; the effect of this factor is equal to the difference between previous and current experiment) to simulate the impacts of individual environmental factors on N_2O fluxes. In total, seven experiments (from S0 to S6) were designed (Figure 4). The S0 reference (baseline) run was designed to track the model internal fluctuation and model drift. The S1 experiment included the temporal variations of all time-varying driving forces. "Best estimate" of N_2O emissions were acquired from either S1 experiment (for models considering

manure as input) or S2 experiment (for models without considering manure). The overall effect of all environmental factors was calculated as: S1-S0. The effects of manure N use (MANN), N fertilizer use (NFER), N deposition (NDEP), LCLU, atmospheric CO_2 (CO_2), and climate (CLIM) were respectively calculated as: S1−S2, S2−S3, S3−S4, S4−S5, S5−S6, and S6−S0, respectively.

7. Model outputs, quality control and data availability

All participating model groups are requested to provide the gridded simulations of N_2O fluxes from global terrestrial ecosystems and other relevant variables that can be used for understanding C-N coupling and key N processes simulated by each individual model (Table 4). The required model output will be submitted at the annual time-step during 1860-2015 and at the monthly time-step during 1980-2015. In addition to modeling estimates of grid-level fluxes and pool sizes, modeling groups will submit biome-level results to facilitate biome-level N_2O emission analysis and split contributions of global N_2O dynamics to primary biome types. The model output from each modeling group is sent to the core team led by Dr. Hanqin Tian for data quality checking and preliminary analysis. The quality control is conducted to check if the individual model results are reasonable and to avoid the obvious errors during model simulations. After quality control process, model output is transferred to a data sharing website.

The model input and output datasets are made available to all model groups for further analyses. Model input data and model results will be made available to broader research community once the results of the first NMIP are published. A data use and authorship policy has been established.

8. Result analysis and synthesis

Based on model results, the NMIP team will provide multi-model ensemble estimates for terrestrial N_2O fluxes at various scales from country-, sector-, continental, to global, and also assess differences and uncertainties among participating models. Through the seven simulation experiments, the magnitudes and spatiotemporal variations in terrestrial N_2O emissions will be attributed to changes in different environmental factors at both regional and global scales. The global and regional N_2O flux data derived from other sources including atmospheric inversion, statistical extrapolation, and inventory approaches (e.g., the N_2O emission data collected in Tian et al. 2016) will be compared and integrated with the NMIP modeled results. Through these syntheses and evaluations of modeled versus field observed N_2O dynamics, we will further identify the gaps in our understanding to estimate N_2O fluxes and put forward potential strategies to improve the models. In the following sections, we provide an initial analysis of simulated terrestrial N_2O emissions from the three models (DLEM, O-CN, and VISIT), which simulate both natural and agricultural emissions.

As indicated by the model ensemble, the global N_2O emission has significantly increased, especially since the 1960s with more rapidly rising exogenous N inputs to terrestrial ecosystems (Figure 5). Natural soils were the largest source across the entire period. Cropland is the single largest contributor to the increasing trend in N_2O emissions during 1860-2015. Despite the same input datasets, the interannual variations among the three models were different due to the differences in model structure and parameters. The estimated N_2O emissions from VISIT were consistently higher than those from the other two models during 1860-2015; N_2O emissions from DLEM and O-CN were similar in magnitude. The increasing trends of N_2O emissions before the end of 1960s were similar among the three models, while the largest increasing trend was found for O-CN, followed by DLEM and the least for VISIT. The ultimate global terrestrial N_2O

budgets, interannual variations, and attributions of the differences among models will be further analyzed in more detail after modeling results from all ten models are included.

The terrestrial N_2O emissions showed substantial spatial variations across the global land surface since 1860 (Figure 6). The highest emission was from the tropical area during all four periods (i.e., the 1860s, 1900s, 1950s, and 2001-2015) (Figure 6), primarily due to higher soil N transformation rates and soil N contents in tropical ecosystems. The latitudinal distribution patterns were slightly different from the 1860s to 2001-2015, showing an increasing importance and second peak of N_2O emissions in the temperate climatic zone of the Northern Hemisphere. Temperate regions were another hotspot for N_2O emissions due to the high N fertilizer use and N deposition rates in China, India, Europe, and the contiguous United States. Of all 14 examined regions as defined by Global Carbon Project (GCP) CH_4 budget synthesis (Saunois et al., 2016), tropical South America had the largest N_2O emissions throughout the study period, contributing to about 20% of the global total emission (Figure 7). China and the contiguous United States were characterized by the most rapid N_2O increasing rates. In the recent three decades, China, India, and western Europe were the only three regions with higher N_2O emissions from cropland than that from natural ecosystems. It is noteworthy to point out that the estimated cropland N_2O emissions in these three regions have large uncertainty ranges due to varied model representation and parameterization methods of the impacts from agricultural management. Larger uncertainty ranges for N_2O emissions from natural ecosystems were found in Russia, Northern Africa, Boreal North America, Southeast Asia, and the contiguous United States.

9. Summary

Current assessments of terrestrial N_2O emission at regional and global scales are subject to large uncertainties. The NMIP is attempting to better identify, and eventually reduce those uncertainties. The activity was initialized in 2015 and currently includes ten terrestrial biosphere models with N cycling coupled. NMIP is an open initiative and other models are invited to join the effort. It targets to provide an improved estimate of global and regional terrestrial N_2O fluxes as a contribution to the larger GCP Global N_2O Budget activity. NMIP is being developed with the capacity to update flux estimates at regular intervals and quantify the uncertainties related to model structure, algorithms, and parameters. The NMIP protocol includes seven simulation experiments to quantify and attribute the contribution of environmental factors to the inter-annual variation and long-term trend of terrestrial N_2O emissions. In addition, this project intends to identify our knowledge gaps and bring forward potential strategies for improving the prediction capability of N_2O models in the future. The data products and ensemble estimates of terrestrial N_2O emissions will be made available and package to be relevant for policy makers and non-government entities participating in the climate change issues.

Acknowledgments

H. Tian and his team acknowledge the support by National Key Research and Development Program of China (# 2017YFA0604702), CAS Grants (KFJ-STS-ZDTP-0; SKLURE2017-1-6), NOAA Grants (G00010410, G00010318), National Science Foundation (1210360, 1243232) and Auburn University IGP Program. A. Ito was supported by Japan Society for the Promotion of Science (Grant # 17H01867). C. Peng acknowledges the support by National Science and Engineering Research Council of Canada (NSERC) discovery grant and China's QianRen Program. E. Saikawa was supported by NOAA Climate Program Office's AC4 program, award #

NA13OAR4310059. S. Zaehle was supported by the European Research Council (ERC) under the European Union's H2020 Programme (grant # 647304; QUINCY). P. Ciais and J. Chang are supported by the European Research Council Synergy grant ERC-2013-SyG-610028 IMBALANCE-P. S. Lienert and F. Joos acknowledge support by the Swiss National Science Foundation (# 200020_172476). We acknowledge Dr. Andy Jacobson for extending global gridded monthly CO_2 data for us to use in the NMIP. The authors declare no conflict of interest.

Appendix A: Brief description of algorithms associated with N_2O flux in each participating model

1) CLM-CN-N_2O:

CLMCN-N_2O is based on the DeNitrification-DeComposition (DNDC) model (Li et al., 1992) implemented in the Community Land Model v3.5 (Oleson et al., 2008; Stöckli et al., 2008) with explicit carbon and nitrogen (CN) processes (Thornton et al., 2007; Randerson et al., 2009; Thornton et al. 2009). CLMCN-N_2O is added to CLM-CN v3.5 in a one-way coupling framework and simulates N_2O emissions during nitrification and denitrification processes at an hourly time step.

Nitrification (R_{nit}) is temperature and moisture dependent and N_2O is computed by the following equation as described in Li et al. (1992):

$$R_{nit} = C_{NH4} f(T1) \quad (1)$$

where C_{NH4} is the NH_4^+-N content in soil and $f(T1)$ is the response function of soil temperature to nitrification rate.

Denitrification is also soil temperature and moisture dependent and it takes place under the anaerobic state. CLMCN-N_2O specifies the anaerobic state when the water-filled pore space is more than 41.5% in the soil layer. Under this condition, N_2O is created based on the growth rate of denitrifying bacteria, as well as consumption and assimilation by plants and microbes, following Li et al. (1992). Detailed processes in simulating N_2O emissions can be found in Saikawa et al., 2013.

2) DLEM2.0:

The nitrogen cycle scheme in DLEM2.0 (Yang et al. 2015; Xu et al. 2017) are similar as DLEM1.0 (Tian et al., 2010, 2011, 2012; Lu and Tian., 2013; Xu et al., 2012), However, the N_2O emission schemes in DLEM2.0 (Xu et al., 2017) have been modified based on Chatskikh et al. (2005) and Heinen (2006).

$$R_{nit} = k_{nit\_max} f(T1) f(WFPS) C_{NH4} \quad (2)$$

$$R_{den} = k_{den\_max} f(T2) f(WFPS) C_{NO3} \quad (3)$$

where R_{nit} is the daily nitrification rate (g N/m^2/d); R_{den} is the daily denitrification rate (g N/m^2/d); $f(T1)$ and $f(T2)$ are the impact function of daily soil temperature on nitrification and denitrification, respectively; $f(WFPS)$ is the impact function of water-filled pore space (WFPS) on nitrification, denitrification and N_2O diffusion; k_{nit_max} is the maximum fraction of NH_4^+-N that is converted to NO_3^--N or gases (0-1); k_{den_max} is the maximum fraction of NO_3^--N that is converted to gases (0-1); C_{NH4} and C_{NO3} are the soil NH_4^+-N and NO_3^--N content (g N/m^2). N_2O from denitrification and nitrification processes are calculated as,

$$R_{N2O} = (R_{nit} + R_{den}) f(T3)(1 - f(WFPS)) \quad (4)$$

where R_{N2O} is the daily N_2O emission rate (g N/m^2/d); $f(T3)$ is the impact function of daily soil temperature on N_2O diffusion rate from soil pores. The calculation methods for these functions and parameters were described in detail in Xu et al. (2017) and Yang et al. (2015).

3) LM3V-N:

In LM3V-N, nitrification is proportional to substrate availability (i.e., NH_4^+), modified by functions that account for effects of temperature and WFPS adapted from Parton et al. (1996). Nitrification-associated N_2O emission (R_{nit}) is evaluated by

$$R_{nit} = k_{nit\_base} f(WFPS) f(T1) C_{NH4} / b_{NH4} \quad (5)$$

where k_{nit_base} is the base nitrification rate; b_{NH4} is the buffer parameter for soil NH_4^+.

Denitrification is described by a Monod-type equation, where both carbon and nitrate substrate availability can have limiting effects on N gas production following Li et al. (2000). These functions are further modified by temperature (based on Xu-Ri and Prentice, 2008), and by WFPS indicating the availability and/or absence of oxygen (adapted from Parton et al., 1996).

$$R_{den} = k_{den\_base} f(T2) f(WFPS) f_g C_{NO3} / b_{NO3} \quad (6)$$

where k_{den_base} is the base denitrification rate; f_g denotes the impact of labile carbon availability to nitrate on the growth of denitrifies; b_{NO3} is the buffer parameter for soil NO_3^-.

Gaseous losses are partitioned between NO_x and N_2O during nitrification is parameterized based on air-filled porosity, following Parton et al. (2001). Partitioning between N_2O and N_2 during denitrification follows the empirical function of Del Grosso et al. (2000), which combines effects of substrate, electron donors (labile C), and water filled pore space.

$$R_{N2O} = 0.004 R_{nit} + R_{den} f(WFPS) f(C_{NO3}) \quad (7)$$

Nitrification/denitrification are treated as fast processes (Shevliakova et al., 2009) and thus updated on sub-hourly time steps along with updates on soil moisture, soil temperature and C and N mineralization. Model description including model formulation are detailed in Huang and Gerber (2015).

4) LPJ-GUESS:

The nitrogen cycle scheme in LPJ-GUESS is based on CENTURY (Parton et al., 1996) and Xu-Ri and Prentice (2008). Inorganic soil nitrogen pools in the model are: ammonium, nitrite and nitrate. Nitrification only occurs in the dry part of the soil (fractionated using water-filled pore space, WFPS), the ratio between N_2O and NO_x of the gaseous losses in nitrification is based on the moisture content in the soil (f(WFPS)).

$$R_{nit} = k_{nit\_max} f(WFPS) C_{NH4} \quad (8)$$

Denitrification occurs in the wet part (based on WFPS) of the soil, the denitrification rate depends on temperature, soil moisture and labile carbon (approximated with heterotrophic respiration, rh). Gaseous losses through denitrifcation results in N_2O, N_2 and NO_x.

$$R_{den} = k_{den\_base} f(T2) f(WFPS) f(rh) C_{NO3} \quad (9)$$

The fractionation between the gaseous N species are modelled using soil moisture and temperature. All losses of gaseous N, are modelled. Emissions to the atmosphere from these pools are modelled using rate modifiers that are based on the soil moisture and temperature. No re-transformation of these gaseous N species is considered. These processes (N-cycling and gaseous N emissions) are modelled in different land use classes: natural vegetation, pastures/rangelands and croplands. On croplands, fertilizers are spread as mineral and/or organic N. Mineral fertilizers are considered as an input to the ammonium and nitrate pools at a fixed

ratio (50/50), and manure as an input into the organic nitrogen pool with a fixed C:N ratio (currently set to 30).

5) LPX-Bern:

The implementation of nitrogen dynamics in LPX-Bern is based on the work of Xu-Ri and Prentice (2008). Nitrogen uptake by plants is governed by their demand and the availability of nitrogen in two soil pools representing ammonium and nitrate. Nitrogen from deposition and fertilization are added to these inorganic soil pools. Losses include ammonium volatilization, nitrate leaching as well as N_2O and NO production during nitrification and N_2O, NO and N_2 production during denitrification. Aerobic nitrification of ammonium is dependent on soil temperature (T_{soil}) and indirectly on soil water content due to the partitioning of wet and dry soil:

$$R_{nit} = max_{nit} f_1(T_{soil}) C_{NH4,dry} \quad (10)$$

where $max_{nit} = 0.92\ \text{day}^{-1}$ is the daily maximum nitrification rate at 20°C.

Anaerobic denitrification of nitrate in wet soil depends on labile carbon availability and soil temperature:

$$R_{den} = R_{mb}/(R_{mb} + K_{mb}) f_2(T_{soil}) C_{NO3,wet}/(C_{NO3,wet} + K_n) \quad (11)$$

The parameters K_{mb} and K_n are taken from Xu-Ri and Prentice (2008) and R_{mb} is the microbiotical soil respiration. The amount of Nitrogen lost as N_2O due to nitrification and denitrification is modelled as a function of soil temperature, water content and the respective process rate.

6) O-CN:

The treatment of inorganic soil nitrogen dynamics in O-CN follows largely Xu-Ri and

Prentice (2008). O-CN (Zaehle and Friend, 2010) considers N losses to NH_3 volatilisation, NOx, N_2O and N_2 production and emission, as well as NH_4 and NO_3 leaching. Inorganic nitrogen dynamics in the soil are tightly coupled to plant uptake and net mineralization. The anaerobic volume fraction of the soil is estimated by an empirical function of the fractional soil moisture content (Zaehle et al. 2011). The fraction of ammonium in the aerobic part of the soil is subject to nitrification, according to:

$$R_{nit} = vmax_{nit} f(T1) f(pH1) C_{NH4} \quad (12)$$

where *f(pH1)* is the soil pH response functions for nitrification (Li et al. 1992; Xu-Ri and Prentice, 2008), and $vmax_{nit}$ is the maximum daily nitrification rate under 20°C and favourable pH conditions (Xu-Ri and Prentice, 2008).

Gross denitrification of the fraction of nitrate under anoxic conditions is modelled as:

$$R_{den} = R_{mb}/(R_{mb} + K_{mb}) f(T2) f(pH2) C_{NO3}/(C_{NO3} + K_n) \quad (13)$$

where *f(pH2)* is the soil pH response functions for denitrification (Li et al., 1992; Xu-Ri and Prentice, 2008), R_{mb} is the soil microbial respiration rate, and K_{mb} and K_n parameters taken from Li et al. (1992).

The N_2O production from nitrification and denitrifcation is then calculated as:

$$R_{N2O} = a_{nit} f(T1) R_{nit} + b_{den} f(T2) f(pH3) R_{den} \quad (14)$$

where a_{nit} and b_{denit} are fraction loss constants, *f(pH3)* is a pH-modifier changing the degree of denitrification producing N_2O versus NO_x or N_2 (Zaehle et al. 2011). Emissions of volatile compounds are simulated using the empirical emission of Xu-Ri and Prentice (2008).

7) ORCHIDEE:

589 Modeling of the mineral N dynamics by the ORCHIDEE model originates from the
590 formulations used in the O-CN (Zaehle and Friend, 2010). It is composed of five pools for
591 ammonium/ammoniac, nitrate, NOx, nitrous oxide, and di-nitrogen forms. N_2O production in
592 both nitrification and denitrification processes are represented.

593 The potential daily rate of nitrification, R_{nit}, occurs only on the aerobic fraction of the
594 soil and is a function of temperature, pH, and ammonium concentration (C_{NH4}):

595 $$R_{nit} = (1 - f(WFPS))f(T1)f(pH1)k_{nit}C_{NH4} \quad (15)$$

596 where k_{nit} is the reference potential $NO3^-$ production per mass unit of ammonium.

597 N_2O production by nitrification ($R_{N2O,nit}$, g N-N_2O/m^2/d) is expressed as a function of the
598 potential daily rate of nitrification (R_{nit}, g N-NO_3^-/m^2/d), temperature and the water content as
599 shown in Zhang et al. (2002).

600 $$R_{N2O,nit} = f(WFPS)f(T1)R_{nit}p_{N2O,nit} \quad (16)$$

601 where $p_{\text{N2O,nit}}$ (g N-N_2O (g N-NO_3^-)$^{-1}$) is the reference N_2O production per mass unit of NO_3^-
602 produced by nitrification.The denitrification occurs on the anaerobic fraction of the soil which is
603 computed as a function of the water-filled porosity (f(*WFPS*)) and is controlled by temperature,
604 pH, soil NO concentration and denitrifier microbial activity (a_{microb}, g m^{-2}) (Li et al., 2000).

605 $$R_{N2O,den} = f(WFPS)f(T2)f(pH)f(NO)p_{N2O,den}a_{microb} \quad (17)$$

606 where *f(NO)* is a Michaelis-Menten shape function and $p_{N2O,den}$ is the reference N_2O production
607 per mass unit of denitrifier microbes.

608

609 8) ORCHIDEE-CNP

610 ORCHIDEE-CNP (Goll et al., 2017) is a version with the implementation of the
611 phosphorus cycle into the nitrogen enabled version of ORCHIDEE (ORCHIDEE-CN; Vuichard

612 in prep.). The inorganic soil nitrogen dynamics of ORCHIDEE-CNP includes N_2O from both
613 nitrification and denitrification processes following the processes of O-CN (Zaehle et al., 2011).
614 One exception is the BNF. In ORCHIDEE-CNP, BNF is a function of NPP (Cleveland et al.,
615 1999) and also regulated by soil mineral N concentration. ORCHIDEE-CNP accounts for
616 influence of phosphorus state of vegetation on tissue nutrient concentrations and phosphatase-
617 mediated biochemical mineralization. Changes in nutrient content (quality) of litter affect the
618 carbon use efficiency of decomposition and in return the nutrient availability to vegetation. The
619 model explicitly accounts for root zone depletion of phosphorus as a function of root phosphorus
620 uptake and phosphorus transport from soil to the root surface.
621
622 9) TRIPLEX-GHG
623 TRIPLEX-GHG model (Zhu et al., 2014; Zhang et al., 2017) is designed to simulate N_2O
624 emissions by coupling major theoretical foundations for processes of nitrification and
625 denitrification reported by Li et al. (2000). Briefly, the nitrification rate is calculated by the
626 Michaelis-Menten function based on the concentration of NH_4^+, and microbial activity of
627 nitrifying bacteria is explicitly involved based on simulating their growth and death;
628 denitrification is expressed in a more complex way by taking into account the chain reaction
629 ($NO_3^- \rightarrow NO_2^- \rightarrow NO \rightarrow N_2O \rightarrow N_2$). Each step of denitrification can be regarded as an
630 independent process, but these steps are linked by competition for DOC between specific
631 denitrifiers during each step. A double substrate-based (DOC and NO_x) Michaelis-Menten
632 equation was adopted to simulate the growth rates of NO_x denitrifiers (Li et al., 2000). In
633 addition, the effects of different factors, such as soil temperature, soil moisture and pH, are also
634 considered. The key equations for nitrification are showed as follows,

635 $$R_{nit} = B_{nit} \frac{R_{max} C_{NH4}}{(6.18+C_{NH4})} pH \quad (18)$$

636 $$R_{max} = COE_{NR} \cdot N_p \quad (19)$$

637 $$F_{NN2O} = FMAX_{N2O} R_{nit} f(T1) f(WFPS) \quad (20)$$

638 where R_{nit} is the nitrification rate (kg N m^{-2} d^{-1}); R_{max} is the maximum nitrification rate (d^{-1}); B_{nit}
639 is the biomass concentration of nitrifiers (kg C m^{-2}); *pH* is the soil pH; COE_{NR} represents the
640 nitrification coefficient; N_p represents the nitrification potential (mg N kg^{-1} d^{-1}); $FMAX_{N2O}$ is the
641 maximum N_2O fraction during nitrification (kg N m^{-2} d^{-1}); and *f(T1)* and *f(WFPS)* are the
642 functions of the effects of soil temperature and soil moisture on N_2O emissions during
643 nitrification, respectively.

644 The key equations for denitrification are showed as follows,

645 $$R_{NOX} = MUE_{NOX} \frac{[DOC]}{[DOC]+K_c} \frac{[NO_x]}{[NO_x]+K_n} \quad (21)$$

646 $$F_{ANNOX} = COE_{dNOx} B_{denit} \left(\frac{R_{NOx}}{EFF_{NOx}} + \frac{MAI_{NOx}[NO_x]}{[N]} \right) f_{NOx}(pH2) f(T2) \quad (22)$$

647 where MUE_{NOx} is the maximum growth rate of NO_x denitrifiers (h^{-1}); [DOC] and [NO_x] represent
648 the concentrations of DOC (kg C m^{-3} h^{-1}) and NO_x (kg N m^{-3} h^{-1}), respectively, in the anaerobic
649 balloon; K_c (kg C m^{-3}) and K_n (kg N m^{-3}) are the half saturation value of C and N oxides,
650 respectively. F_{ANNOX} is the consumption rate of NO_x (kg N m^{-3} h^{-1}); COE_{dNOx} represents the
651 coefficient of NO_x consumption; B_{denit} is the biomass of denitrifiers (kg C m^{-3}); R_{NOx} is the NO_x
652 reduction rate (h^{-1}); [NO_x] and [N] are the concentrations of NO_x and total N, respectively, in the
653 anaerobic balloon (kg N m^{-3}); EFF_{NOx} is the efficiency parameter for NO_x denitrifiers (kg C kg N
654 $^{-1}$); MAI_{NOx} is the maintenance coefficient of NO_x (h^{-1}); and $f(t)_{denit}$ represents the effect of the
655 soil temperature on the denitrification rate during each step.

656

10) VISIT

The nitrogen cycle scheme of VISIT is composed of three organic soil nitrogen pools (microbe, litter, and humus), two inorganic soil nitrogen pools (ammonium and nitrate), and vegetation pools. Fertilizer is considered as an input to the ammonium and nitrate pools at a fixed ratio, and manure as an input into the litter organic nitrogen pool. N_2O emissions through nitrification and denitrification are estimated using the scheme developed by Parton et al. (1996). Nitrification-associated N_2O emission ($R_{nit,N2O}$) is evaluated as follows,

$$R_{nit,N2O} = f(WFPS)f(pH1)f(T1)(K_{max} + F_{max}f(NH4)) \quad (23)$$

where K_{max} is the soil-specific turnover coefficient; F_{max} is the parameter of maximum nitrification gas flux; and $f(NH_4)$ is the effect of soil ammonium on nitrification. Denitrification-associated N_2O emission ($R_{den,N2O}$) is evaluated by the following equation:

$$R_{den,N2O} = R_{den}(1 + R_{N2/N2O}) \quad (24)$$

$$R_{den} = \min(f(NO_3), f(CO_2)) \times f(WFPS) \quad (25)$$

where $R_{N2/N2O}$ is the fractionation coefficient, which is also a function of WFPS, soil nitrate, and heterotrophic respiration, $f(NO_3)$ is the maximum denitrification rate in high soil respiration rate condition, $f(CO_2)$ is the maximum denitrification rate in high NO_3^- levels, and $f(WFPS)$ is the effect of WFPS on denitrification rate.

References

Battaglia, G. and Joos, F. In PRESS: Marine N_2O emissions from nitrification and denitrification constrained by modern observations and projected in multi-millennial global warming simulations. Global Biogeochemical Cycles. **DOI:** 10.1002/2017GB005671 Bonan, G. B. 2001: Observational evidence for reduction of daily maximum temperature by croplands in the Midwest United States. Journal of Climate, 14(11), 2430-2442.

Brotto, A. C., Kligerman, D. C., Andrade, S. A., Ribeiro, R. P., Oliveira, J. L., Chandran, K., and de Mello, W. Z, 2015: Factors controlling nitrous oxide emissions from a full-scale activated sludge system in the tropics, Environmental Science and Pollution Research, 22, 11840-11849.

Butterbach-Bahl, K., Baggs, E. M., Dannenmann, M., Kiese, R., and Zechmeister-Boltenstern, S., 2013: Nitrous oxide emissions from soils: how well do we understand the processes and their controls?, Philosophical Transactions of the Royal Society B, 368, 20130122, https://doi.org/10.1098/rstb.2013.0122.

Cai, Z., Xing, G., Yan, X., Xu, H., Tsuruta, H., Yagi, K., and Minami, K., 1997: Methane and nitrous oxide emissions from rice paddy fields as affected by nitrogen fertilisers and water management, Plant and soil, 196, 7-14.

Chatskikh, D., Olesen, J. E., Berntsen, J., Regina, K., and Yamulki, S., 2005: Simulation of effects of soils, climate and management on N_2O emission from grasslands, Biogeochemistry, 76, 395-419.

Ciais, P., and Coauthors, 2013: Carbon and other biogeochemical cycles. In Climate Change 2013: The Physical Science Basis. Contribution of Working Group I to the Fifth Assessment Report of the Intergovernmental Panel on Climate Change, Cambridge University Press, Cambridge, UK, 465–570.

Cleveland, C. C. and Coauthors, 1999: Global patterns of terrestrial biological nitrogen (N_2) fixation in natural ecosystems, Global Biogeochemical Cycles, 13, 623-645.

Davidson, E. Keller, M., Erickson, H., Verchot, L., and Veldkamp, E., 2000: Testing a conceptual model of soil emissions of nitrous and nitric oxides: using two functions based on soil nitrogen availability and soil water content, the hole-in-the-pipe model characterizes a large fraction of the observed variation of nitric oxide and nitrous oxide emissions from soils. AIBS Bulletin 50, 8(2000), 667-680.

Davidson, E. A., 2009: The contribution of manure and fertilizer nitrogen to atmospheric nitrous oxide since 1860, Nature Geoscience, 2, 659-662.

Davidson, E. A. & Kanter, D., 2014: Inventories and scenarios of nitrous oxide emissions. Environ. Res. Lett. 9, 105012.

Del Grosso, S., Parton, W., Mosier, A., Ojima, D., Kulmala, A., and Phongpan, S., 2000: General model for N_2O and N_2 gas emissions from soils due to dentrification, Global Biogeochemical Cycles, 14, 1045-1060.

Ding, W., Yagi, K., Cai, Z., and Han, F., 2010: Impact of long-term application of fertilizers on N_2O and NO production potential in an intensively cultivated sandy loam soil, Water, Air, & Soil Pollution, 212, 141-153.

Eyring, Veronika and Coauthors, 2013: Overview of IGAC/SPARC Chemistry-Climate Model Initiative (CCMI) community simulations in support of upcoming ozone and climate assessments, SPARC newsletter 40(Januar): 48-66.

Firestone, M. K. and Davidson, E. A., 1989: Microbiological basis of NO and N_2O production and consumption in soil, Exchange of trace gases between terrestrial ecosystems and the atmosphere, 47, 7-21.

Fowler, D. and Coauthors, 2013: The global nitrogen cycle in the twenty-first century. Philosophical Transactions of the Royal Society B: Biological Sciences, 368, 20130164–20130164. https://doi.org/10.1098/rstb.2013.0164

Fowler, D. and Coauthors, 2015: Effects of global change during the 21st century on the nitrogen cycle, Atmospheric Chemistry and Physics, 15(24), 13849-13893.

Galloway, J. N. and Coauthors, 2004: Nitrogen Cycles: Past, Present, and Future. Biogeochemistry 70: 153–226

Galloway, J. N. and Coauthors, 2008: Transformation of the nitrogen cycle: recent trends, questions, and potential solutions, Science, 320, 889-892.

Goldberg, S. D. and Gebauer, G., 2009: Drought turns a Central European Norway spruce forest soil from an N_2O source to a transient N_2O sink, Global Change Biology, 15, 850-860.

Goll, D. S. and Coauthors, 2017: A representation of the phosphorus cycle for ORCHIDEE, Geoscientific Model Development Discussion, https://doi.org/10.5194/gmd-2017-62, in review.

737 Gruber, N. and Galloway, J. N., 2008: An Earth-system perspective of the global nitrogen cycle,
738 Nature, 451, 293-296.
739 Heinen, M., 2006: Simplified denitrification models: overview and properties, Geoderma, 133,
740 444-463.
741 Huang, Y. and Gerber, S., 2015: Global soil nitrous oxide emissions in a dynamic carbon-
742 nitrogen model, Biogeosciences, 12, 6405-6427.
743 Huntzinger, D. N. and Coauthors, 2013: The North American Carbon Program Multi-scale
744 Synthesis and Terrestrial Model Intercomparison Project: Part 1: Overview and experimental
745 design, Geoscientific Model Development, 6, 2121–2133, http://doi.org/10.5194/gmd-6-
746 2121-2013.
747 Ichii, K. and Coauthors, 2013: Site-level model–data synthesis of terrestrial carbon fluxes in the
748 CarboEastAsia eddy-covariance observation network: toward future modeling efforts,
749 Journal of Forest Research, 18, 13-20.
750 Inatomi, M., Ito, A., Ishijima, K., and Murayama, S., 2010: Greenhouse gas budget of a cool-
751 temperate deciduous broad-leaved forest in Japan estimated using a process-based model,
752 Ecosystems, 13, 472-483.
753 Ito, A. and Inatomi, M., 2012: Use of a process-based model for assessing the methane budgets
754 of global terrestrial ecosystems and evaluation of uncertainty, Biogeosciences, 9, 759-773
755 Ito, A., Nishina, K., and Noda, H. M., 2016: Evaluation of global warming impacts on the carbon
756 budget of terrestrial ecosystems in monsoon Asia: a multi-model analysis, Ecological
757 research, 31, 459-474.
758 Jung, M., Henkel, K., Herold, M., and Churkina, G., 2006: Exploiting synergies of global land
759 cover products for carbon cycle modeling, Remote Sensing of Environment, 101, 534-553.
760 Klein Goldewijk, K., Beusen, A., Doelman, J., and Stehfest, E., 2016: New anthropogenic land
761 use estimates for the Holocene; HYDE 3.2, Earth System Science Data Discussions,
762 https://doi.org/10.5194/essd-2016-58, in review.
763 Kurokawa, J., Ohara, T., Morikawa, T., Hanayama, S., Janssens-Maenhout, G., Fukui, T.,
764 Kawashima, K., and Akimoto, H. 2013: Emissions of air pollutants and greenhouse gases
765 over Asian regions during 2000–2008: Regional Emission inventory in ASia (REAS) version
766 2. Atmospheric Chemistry and Physics, 21, 11019-11058.

767 Le Quéré, C. and Coauthors, 2016: Global carbon budget 2016, Earth System Science Data, 8,
768 605-649.
769 Li, C., Aber, J., Stange, F., Butterbach-Bahl, K., Papen, H., Zechmeister-Boltenstern, S., Li, C.
770 S., and Aber, J., 2000: A process-oriented model of N_2O and NO emissions from forest soils:
771 1. Model development, Journal of Geophysical Research: Atmospheres, 105, 4369-4384.
772 Li, C., Frolking, S., and Frolking, T. A., 1992: A model of nitrous oxide evolution from soil
773 driven by rainfall events: 1. Model structure and sensitivity, Journal of Geophysical Research:
774 Atmospheres, 97, 9759-9776.
775 Lu, C. and Tian, H., 2017: Global nitrogen and phosphorus fertilizer use for agriculture
776 production in the past half century: shifted hot spots and nutrient imbalance, Earth System
777 Science Data, 9, 181-192.
778 Lu, C. and Tian, H., 2013: Net greenhouse gas balance in response to nitrogen enrichment:
779 perspectives from a coupled biogeochemical model, Global Change Biology, 19, 571-588.
780 Lü, C. and Tian, H., 2007: Spatial and temporal patterns of nitrogen deposition in China:
781 synthesis of observational data, Journal of Geophysical Research: Atmospheres, 112,
782 D22S05, http://doi.org/10.1029/2006JD007990.
783 MacFarling, M. and Coauthors, 2006: Law Dome CO_2, CH_4 and N_2O ice core records extended
784 to 2000 years BP. Geophysical Research Letters, 33. L14810.
785 Melillo, J., Borchers, J., and Chaney, J., 1995: Vegetation/ecosystem modeling and analysis
786 project: Comparing biogeography and geochemistry models in a continental-scale study of
787 terrestrial ecosystem responses to climate change and CO_2 doubling, Global Biogeochemical
788 Cycles, 9, 407-437.
789 Melton, J. and Coauthors, 2013: Present state of global wetland extent and wetland methane
790 modelling: conclusions from a model intercomparison project (WETCHIMP),
791 Biogeosciences, 10, 753-788.
792 Myhre, G., and Coauthors, 2013 Anthropogenic and Natural Radiative Forcing, in: Climate
793 Change 2013: The Physical Science Basis. Contribution of Working Group I to the Fifth
794 Assessment Report of the Intergovernmental Panel on Climate Change, Cambridge
795 University Press, Cambridge, United Kingdom and New York, NY, USA

Oleson, K. and Coauthors, 2008: Improvements to the Community Land Model and their impact on the hydrological cycle, Journal of Geophysical Research: Biogeosciences, 113, G01021, http://doi.org/10.1029/2007JG000563.

Olin, S. and Coauthors, 2015: Soil carbon management in large-scale Earth system modelling: implications for crop yields and nitrogen leaching, Earth System Dynamics, 6, 745-768.

Pan, S. and Coauthors, 2015: Responses of global terrestrial evapotranspiration to climate change and increasing atmospheric CO_2 in the 21st century, Earth's Future, 3, 15-35.

Parton, W., Holland, E., Del Grosso, S., Hartman, M., Martin, R., Mosier, A., Ojima, D., and Schimel, D., 2001: Generalized model for NO_x and N_2O emissions from soils, Journal of Geophysical Research: Atmospheres, 106, 17403-17419.

Parton, W., Mosier, A., Ojima, D., Valentine, D., Schimel, D., Weier, K., and Kulmala, A. E., 1996: Generalized model for N_2 and N_2O production from nitrification and denitrification, Global Biogeochemical Cycles, 10, 401-412.

Parton, W. J., Hartman, M., Ojima, D., and Schimel, D., 1998: DAYCENT and its land surface submodel: description and testing, Global and planetary Change, 19, 35-48.

Potter, C. S., Matson, P. A., Vitousek, P. M., and Davidson, E. A., 1996: Process modeling of controls on nitrogen trace gas emissions from soils worldwide, Journal of Geophysical Research: Atmospheres, 101, 1361-1377.

Potter, C. S., Randerson, J. T., Field, C. B., Matson, P. A., Vitousek, P. M., Mooney, H. A., and Klooster, S. A., 1993: Terrestrial ecosystem production: a process model based on global satellite and surface data, Global Biogeochemical Cycles, 7, 811-841.

Poulter, B. et al. 2017: Global wetland contribution to 2000–2012 atmospheric methane growth rate dynamics, *Environ. Res. Lett.* **12** (2017) 094013. https://doi.org/10.1088/1748-9326/aa8391

Prather, M. J., Holmes, C. D., and Hsu, J., 2012: Reactive greenhouse gas scenarios: Systematic exploration of uncertainties and the role of atmospheric chemistry, Geophysical Research Letter, 39, L09803, https://doi.org/10.1029/2012GL051440.

Prather, M. J. and Coauthors, 2015: Measuring and modeling the lifetime of nitrous oxide including its variability, Journal of Geophysical Research: Atmoshpere, 120, 5693–5705.

Randerson, J. T. and Coauthors, 2009: Systematic assessment of terrestrial biogeochemistry in coupled climate–carbon models, Global Change Biology, 15, 2462-2484.

827 Rice, C. W. and Smith, M. S., 1982: Denitrification in no-till and plowed soils, Soil Science
828 Society of America Journal, 46, 1168-1173.
829 Richardson, A. D. and Coauthors, 2012: Terrestrial biosphere models need better representation
830 of vegetation phenology: results from the North American Carbon Program Site Synthesis,
831 Global Change Biology, 18, 566-584.
832 Rowlings, D., Grace, P., Scheer, C., and Liu, S., 2015: Rainfall variability drives interannual
833 variation in N_2O emissions from a humid, subtropical pasture, Science of The Total
834 Environment, 512, 8-18.
835 Saikawa, E. and Coauthors, 2014: Global and regional emissions estimates for N_2O,
836 Atmospheric Chemistry and Physics, 14, 4617-4641.
837 Saikawa, E., Schlosser, C., and Prinn, R., 2013: Global modeling of soil nitrous oxide emissions
838 from natural processes, Global Biogeochemical Cycles, 27, 972-989.
839 Saunois, M. and Coauthors, 2016: The global methane budget 2000–2012, Earth Syst. Sci. Data,
840 8, 697-751, https://doi.org/10.5194/essd-8-697-2016.
841 Schaefer, K. and Coauthors, 2012: A model-data comparison of gross primary productivity:
842 Results from the North American Carbon Program site synthesis, Journal of Geophysical
843 Research: Biogeosciences, 117, G03010, http://doi.org/10.1029/2012JG001960.
844 Schimel, D. and Coauthors, 2000: Contribution of increasing CO_2 and climate to carbon storage
845 by ecosystems in the United States, Science, 287, 2004-2006.
846 Schmidt, I., van Spanning, R. J., and Jetten, M. S., 2004: Denitrification and ammonia oxidation
847 by Nitrosomonas europaea wild-type, and NirK-and NorB-deficient mutants, Microbiology,
848 150, 4107-4114.
849 Schwalm, C. R. and Coauthors, 2010: A model-data intercomparison of CO_2 exchange across
850 North America: Results from the North American Carbon Program site synthesis, Journal of
851 Geophysical Research: Biogeosciences, 115, G00H05, http://doi.org/10.1029/2009JG001229.
852 Shevliakova, E. and Coauthors, 2009: Carbon cycling under 300 years of land use change:
853 Importance of the secondary vegetation sink, Global Biogeochemical Cycles, 23, GB2022,
854 http://doi.org/10.1029/2007GB003176.
855 Sitch, S. and Coauthors, 2015: Recent trends and drivers of regional sources and sinks of carbon
856 dioxide, Biogeosciences, 12, 653-679.

857 Smith, K. A. and Arah, J., 1990: Losses of nitrogen by denitrification and emissions of nitrogen
858 oxides from soils, Proceedings-Fertilizer Society, UK, 299.
859 Stocker, B. D., Roth, R., Joos, F., Spahni, R., Steinacher, M., Zaehle, S., Bouwman, L., and
860 Prentice, I. C., 2013: Multiple greenhouse-gas feedbacks from the land biosphere under
861 future climate change scenarios, Nature Climate Change, 3, 666-672.
862 Stöckli, R., Lawrence, D., Niu, G. Y., Oleson, K., Thornton, P. E., Yang, Z. L., Bonan, G.,
863 Denning, A., and Running, S. W., 2008: Use of FLUXNET in the Community Land Model
864 development, Journal of Geophysical Research: Biogeosciences, 113, G01025,
865 http://doi.org/10.1029/2007JG000562.
866 Thompson, R. L. and Coauthors, 2014: TransCom N_2O model inter-comparison – Part 2:
867 Atmospheric inversion estimates of N_2O emissions, Atmospheric Chemistry and Physics, 14,
868 6177–6194, https://doi.org/10.5194/acp-14-6177-2014.
869 Thornton, P. E. and Coauthors, 2009: Carbon-nitrogen interactions regulate climate-carbon cycle
870 feedbacks: results from an atmosphere-ocean general circulation model, Biogeosciences, 6,
871 2099-2120.
872 Thornton, P. E., Lamarque, J. F., Rosenbloom, N. A., and Mahowald, N. M., 2007: Influence of
873 carbon-nitrogen cycle coupling on land model response to CO_2 fertilization and climate
874 variability, Global Biogeochemical Cycles, 21, GB4018,
875 http://doi.org/10.1029/2006GB002868.
876 Tian, H. and Coauthors, 2015: Global methane and nitrous oxide emissions from terrestrial
877 ecosystems due to multiple environmental changes, Ecosystem Health and Sustainability, 1,
878 1-20.
879 Tian, H. and Coauthors, 2012: Century-scale responses of ecosystem carbon storage and flux to
880 multiple environmental changes in the southern United States, Ecosystems, 15, 674-694.
881 Tian, H. and Coauthors, 2016: The terrestrial biosphere as a net source of greenhouse gases to
882 the atmosphere, Nature, 531, 225-228.
883 Tian, H., Xu, X., Liu, M., Ren, W., Zhang, C., Chen, G., and Lu, C., 2010: Spatial and temporal
884 patterns of CH_4 and N_2O fluxes in terrestrial ecosystems of North America during 1979-2008:
885 application of a global biogeochemistry model, Biogeosciences, 7, 2673-2694.
886 Tian, H., Xu, X., Lu, C., Liu, M., Ren, W., Chen, G., Melillo, J., and Liu, J., 2011: Net
887 exchanges of CO_2, CH_4, and N_2O between China's terrestrial ecosystems and the atmosphere

and their contributions to global climate warming, Journal of Geophysical Research: Biogeosciences, 116, G02011, http://doi.org/10.1029/2010JG001393.

Vuichard et al., Accounting for carbon and nitrogen interactions in a global terrestrial ecosystem model: Multi-site evaluation of the ORCHIDEE model, in prep.

Wania, R. and Coauthors, 2013: Present state of global wetland extent and wetland methane modelling: methodology of a model inter-comparison project (WETCHIMP), Geoscientific Model Development, 6, 617-641.

Warszawski, L., Frieler, K., Huber, V., Piontek, F., Serdeczny, O., and Schewe, J., 2014: The inter-sectoral impact model intercomparison project (ISI–MIP): project framework, Proceedings of the National Academy of Sciences, 111, 3228-3232.

Wei, Y. and Coauthors, 2014: The North American Carbon Program Multi-scale Synthesis and Terrestrial Model Intercomparison Project – Part 2: Environmental driver data, Geosci. Model Dev., 7, 2875-2893, https://doi.org/10.5194/gmd-7-2875-2014.

Winiwarter, W., Höglund-Isaksson, L ., Klimont, Z., Schöpp, W., Amann, M., 2017: Technical opportunities to reduce global anthropogenic emissions of nitrous oxide Environ. Res. Letters, DOI 10.1088/1748-9326/aa9ec9

Wrage, N., Velthof, G., Van Beusichem, M., and Oenema, O.: Role of nitrifier denitrification in the production of nitrous oxide, Soil biology and Biochemistry, 33, 1723-1732, 2001.

Xu-Ri, and Prentice I. C.: Terrestrial nitrogen cycle simulation with a dynamic global vegetation model. Global Change Biology, 14, 1745-1764, 2008.

Xu, R., Tian, H., Lu, C., Pan, S., Chen, J., Yang, J., and Zhang, B., 2017: Preindustrial nitrous oxide emissions from the land biosphere estimated by using a global biogeochemistry model, Climate of the Past, 13, 977-990, https://doi.org/10.5194/cp-13-977-2017.

Xu, X., Tian, H., Chen, G., Liu, M., Ren, W., Lu, C., and Zhang, C., 2012: Multifactor controls on terrestrial N_2O flux over North America from 1979 through 2010, Biogeosciences, 9, 1351-1366.

Yang, Q., Tian, H., Friedrichs, M. A., Hopkinson, C. S., Lu, C., and Najjar, R. G., 2015: Increased nitrogen export from eastern North America to the Atlantic Ocean due to climatic and anthropogenic changes during 1901–2008, Journal of Geophysical Research: Biogeosciences, 120, 1046-1068.

Zaehle, S., Ciais, P., Friend, A. D., and Prieur, V., 2011: Carbon benefits of anthropogenic reactive nitrogen offset by nitrous oxide emissions, Nature Geoscience, 4, 601-605.

Zaehle, S. and Friend, A., 2010: Carbon and nitrogen cycle dynamics in the O-CN land surface model: 1. Model description, site-scale evaluation, and sensitivity to parameter estimates, Global Biogeochemical Cycles, 24, GB1005, http://doi.org/10.1029/2009GB003521.

Zhang, B., Tian, H., Lu, C., Dangal, S. R. S., Yang, J., and Pan, S., 2017: Manure nitrogen production and application in cropland and rangeland during 1860-2014: A 5-minute gridded global data set for Earth system modeling. Earth System Science Data Discussion, https://doi.org/10.5194/essd-2017-11.

Zhang, K., Peng C.H., Wang M., Zhou X.L., Li M.X., Wang K.F., Ding J.H., and Zhu Q.A., 2017: Process-based TRIPLEX-GHG model for simulating N_2O emissions from global forests and grasslands: Model development and evaluation. Journal of Advances in Modeling Earth Systems, In revision.

Zhang, Y., Li, C., Zhou, X., and Moore, B., 2002: A simulation model linking crop growth and soil biogeochemistry for sustainable agriculture, Ecological Modelling, 151, 75-108.

Zhu, Q. and Coauthors, 2014: Modelling methane emissions from natural wetlands by development and application of the TRIPLEX-GHG model, Geoscientific Model Development, 7, 981-999.

Zhuang, Q., Lu, Y., and Chen, M., 2012: An inventory of global N_2O emissions from the soils of natural terrestrial ecosystems. Atmospheric environment, 47, 66-75.

Figure Captions

Figure 1. The framework of the N_2O Model Intercomparison project (NMIP).

Figure 2. Evolution of the major driving factors at the global level during 1901-2016. (a) Annual temperature (°C, solid line) and annual precipitation (mm, dash line), (b) atmospheric CO_2 concentration (ppm), (c) cropland area (million km^2), (d) N deposition (Tg N yr^{-1}), (e) N fertilizer application (Tg N yr^{-1}) during 1900-2013, and (f) manure N production (Tg N yr^{-1}).

Figure 3. Spatial distribution of N deposition (a, d, g, j; g N m^{-2} yr^{-1}), N fertilizer application (b, e, h, k; g N m^{-2} cropland yr^{-1}), and manure N production (c, f, i, l; g N m^{-2} yr^{-1}) in 1860 (1st row), 1900 (2nd row), 1950 (3rd row), and 2015 (4th row).

Figure 4. Model simulation experimental designs (Note: S0: reference (baseline); S1: CLIM+CO_2+LCLU+NDEP+NFER+MANN; S2: CLIM+ CO_2+LCLU+NDEP+NFER; S3: CLIM+ CO_2+LCLU+NDEP; S4: CLIM+ CO_2+LCLU; S5: CLIM+ CO_2; S6: CLIM). CLIM: climate, CO_2: atmospheric CO_2, LCLU: land cover and land use change, NDEP: N deposition, NFER: N fertilizer use, and MANN: manure N use.

Figure 5. Interannual variations in N_2O emissions from global terrestrial ecosystems during 1861-2015 as estimated by the average of three process-based models (DLEM, O-CN, and VISIT). The gray shades denote ± 1 standard deviation.

Figure 6. Spatial patterns and the latitudinal variations of mean annual N_2O emissions as represented by the mean estimates from DLEM, VISIT, and O-CN models in the (a) 1860s, (b) 1900s, (c) 1950s, and (d) 2001-2015. The pie charts indicate the relative contributions of natural vegetation (blue) and cropland (red) to the total N_2O emissions. The gray shades denote ± 1 standard deviation.

Figure 7. Decadal N_2O emissions (Tg N yr^{-1}) from the natural ecosystems (blue lines) and cropland (red lines) in 14 regions (region delineation is from the Global Carbon Project global CH_4 budget synthesis, Saunois et al., 2016). N_2O emissions are represented by the average of DLEM, VISIT, and O-CN model simulations. The error bars denote ± 1 standard deviation.

Table 1. Summary of the NMIP driving forces

Data name	Period	Temporal resolution	Spatial resolution	Sources	Variables
Climate	1901-2015	6-hourly	0.5°	CRU-NCEP	Incoming longwave / shortwave radiation, air humidity, pressure, precipitation, temperature, and wind speed
CO_2	1860-2015	Monthly	0.5°	NCAR	CO_2 concentration
N deposition	1860-2015	Yearly	0.5°	Eyring et al. (2013)	NH_x-N and NO_y-N deposition
N Fertilizer use	1860-2014	Yearly	0.5°	Lu and Tian (2017)	N fertilizer use rate in cropland
Manure N input	1860-2014	Yearly	0.5°	Zhang et al. (2017)	Manure N production
Potential vegetation	One time	One time	0.5°	SYNMAP	Fraction of natural vegetation types
Cropland	1860-2015	Yearly	0.5°	HYDE 3.2	Cropland fraction

Note: Detailed descriptions of the major NMIP model input datasets have been provided in previous publications or online documents. Here we only provide a brief description of sources and spatiotemporal patterns of these datasets.

987 **Table 2**. Participating models

Model	Full name	Contact	Affiliation	Citation
CLM-CN	Community land model - CN	Eri Saikawa	Emory University, USA	Saikawa et al. (2013)
DLEM	Dynamic Land Ecosystem Model	Hanqin Tian	Auburn University	Tian et al. (2015) Xu et al. (2017)
LM3V-N	Land Model 3V-N	Stefan Gerber	University of Florida	Huang and Gerber (2015)
LPJ-GUESS	Lund-Potsdam-Jena General Ecosystem Simulator	Stefan Olin/ Almut Arneth	Lund University, Sweden/KIM, Dept. Atmospheric Environmental Research, Germany	Olin et al. (2015); Xu-Ri and Prentice (2008)
LPX-Bern	Land Processes and eXchanges model - Bern	Sebastian Lienert/ Fortunat Joos	Institute for Climate and Environmental Physics, University of Bern, Switzerland	Stocker et. al. (2013) Xu-Ri and Prentice (2008)
O-CN	ORCHIDEE-CN	Sönke Zaehle	Max Planck Institute for Biogeochemistry	Zaehle et al. (2011)
ORCHIDEE	Organising Carbon and Hydrology In Dynamic Ecosystems	Nicolas Vuichard	IPSL – LSCE, France	Vuichard et al. (in prep)
ORCHIDEE-CNP	Organising Carbon and Hydrology In Dynamic Ecosystems-CNP	Jinfeng Chang/ Daniel Goll	IPSL – LSCE, France	Goll et al., 2017
TRIPLEX-GHG	TRIPLEX-GHG	Changhui Peng	University of Quebec at Montreal, Canada	Zhu et al. (2014); Zhang et al. (2017)
VISIT	Vegetation Integrated SImulator for Trace-gases	Akihiko Ito	National Institute for Environmental Studies, Japan	Inatomi et al. (2010); Ito and Inatomi (2012)

Table 3. Model characteristics in simulating major N cycling processes

	CLM-CN	DLEM	LM3V-N	LPJ -GUESS	LPX-Bern	O-CN	ORCHIDEE	ORCHIDEE -CNP	TRIPLEX-GHG	VISIT
Open N cycle [1]	yes	yes	yes	yes	yes	yes	yes	yes	yes	yes
C-N coupling	yes	yes	yes	yes	yes	yes	yes	yes	yes	yes
N pools[2]	(13, 3, 4)	(6, 6, 8)	(6, 4, 3)	(5, 6, 11)	(4,3,8)	(9, 6, 9)	(9, 6, 9)	(9, 6, 9)	(3, 9, 4)	(4, 1, 4)
Demand and supply-driven Plant N uptake	yes	yes	yes	yes	yes	yes	yes	yes	yes	yes
N allocation[3]	Dynamic	Dynamic	Dynamic	Dynamic	Dynamic	Dynamic	Dynamic	Dynamic	Dynamic	Dynamic
Nitrification	*f*(T, SWC)	*f*(T, SWC, C_{NH4})	*f*(T, SWC, C_{NH4})	*f*(T, SWC, C_{NH4})	*f*(T, SWC, C_{NH4})	*f*(T, SWC, pH, C_{NH4})	*f*(T, SWC, pH C_{NH4})	*f*(T, SWC, pH, C_{NH4})	*f*(pH, C_{NH4}, T, SWC)	*f*(T, SWC, pH, C_{NH4})
Denitrification	*f*(T, SWC, C_{NO3})	*f*(T, clay, Rh, C_{NO3})	*f*(T_{soil}, Rh, SWC, C_{NH4}, C_{NO3}	*f*(T, Rh, SWC, C_{NO3})	*f*(T, SWC, R_{mb}, C_{NO3})	*f*(T, SWC, pH, R_{mb}, C_{NO3})	*f*(T, SWC, pH, denitrifier, C_{NO3})	*f*(T, SWC, pH, R_{mb}, C_{NO3})	*f*(DOC, C_{NO3}, pH, T_{soil})	*f*(SWC, Rh, C_{NO3})
Mineralization, immobilization	*f*(C:N)	*f*(C:N)	*f*(C_{NO3}, C_{NH4})	*f*(C:N)	*f*(C:N)	*f*(C:N)	*f*(C:N)	*f*(C:N)	*f*(C:N)	*f*(C:N)
N leaching	*f*(runoff)	*f*(runoff)	*f*(runoff)	*f*(runoff)	*f*(runoff)	*f*(runoff, clay)	*f*(runoff)	*f*(runoff)	*f*(runoff)	*f*(runoff)
NH_3 volatilization	*f*(C_{NH4})	*f*(pH, T, SWC, C_{NH4})	*f*(pH, T, SWC, C_{NH4})	*f*(pH, T, SWC, C_{NH4})	*f*(pH, T, SWC, C_{NH4})	*f*(pH, C_{NH4})	*f*(pH,C_{NH4})	*f*(pH,C_{NH4})	*f*(pH, C_{NH4})	*f*(pH, T, SWC, C_{NH4})
Plant N turnover[4]	Dynamic	Dynamic	Dynamic	Dynamic	Dynamic	Dynamic	Dynamic	Dynamic	Dynamic	Dynamic
N resorption	*f*(C:N)	*f*(C:N)	fixed	Crop: dynamic, the rest: fixed	*f*(Nleaf)	fixed	*f*(Nleaf)	fixed	*f*(C:N)	fixed
N fixation	*f*(NPP)	Fixed	*f*(C_{NH4}, C_{NO3}, light, plant demand)	*f*(ET)	*Implied by mass balance*	*f*(C_{cost}, C_{root})	*f*(ET)	*f*(NPP)	*f*(biomass)	*f*(ET)
N fertilizer use	no	yes	yes	yes	yes	yes	yes	yes	yes	yes
Manure N use	no	yes	yes	yes	no	no	yes	yes	no	yes
N deposition	yes	yes	yes	yes	yes	yes	yes	yes	yes	yes

Note: [1] "open" denotes that excess N can be leached from the system; [2]numbers of N pools (vegetation pools, litter pools, soil pools); [3] Dynamic denotes time-varied N allocation ratio to different N pools; [4]turnover time for various vegetation nitrogen pools. T: soil temperature; Clay: soil clay fraction; ET: evapotranspiration; Biomass: vegetation carbon; NPP: net primary production; Nleaf: leaf N concentration; Runoff: soil surface and drainage runoff; Ccost: carbon cost during N_2 fixation; SWC: soil water content; denitrifier: soil denitrifier biomass; Rh: soil heterogeneous respiration.

Table 4. List of nitrogen and carbon variables provided by NMIP models

Name of Variables	Unit	Frequency	Level
Nitrogen Fluxes: N_2O flux, Biological N fixation, Plant N uptake (sum of ammonium and nitrate), Net N mineralization, Nitrification rate, Denitrification rate**,** N leaching (DIN, DON, PON or total N leaching), NH_3 volatilization	kg N m^{-2} s^{-1}	Monthly (1980-2015) Annual (1860-2015)	Grid- and biome-levels
Nitrogen Pools: N in Vegetation, N in Above-ground Litter Pool, N in Soil (including below-ground litter), N in Products pools	kg N m^{-2}	Annual (1860-2015)	Grid-levels
Carbon Fluxes: Gross Primary Production, Autotrophic (Plant) Respiration, Net Primary Production, Heterotrophic Respiration	kg C m^{-2} s^{-1}	Monthly (1980-2015) Annual (1860-2015)	Grid- and biome-levels
Carbon Pools: C in Vegetation, C in Above-ground Litter Pool, C in Soil (including below-ground litter), C in Products pools, C in Vegetation	kg C m^{-2}	Annual (1860-2015)	Grid-level Biome-level (vegetation C)

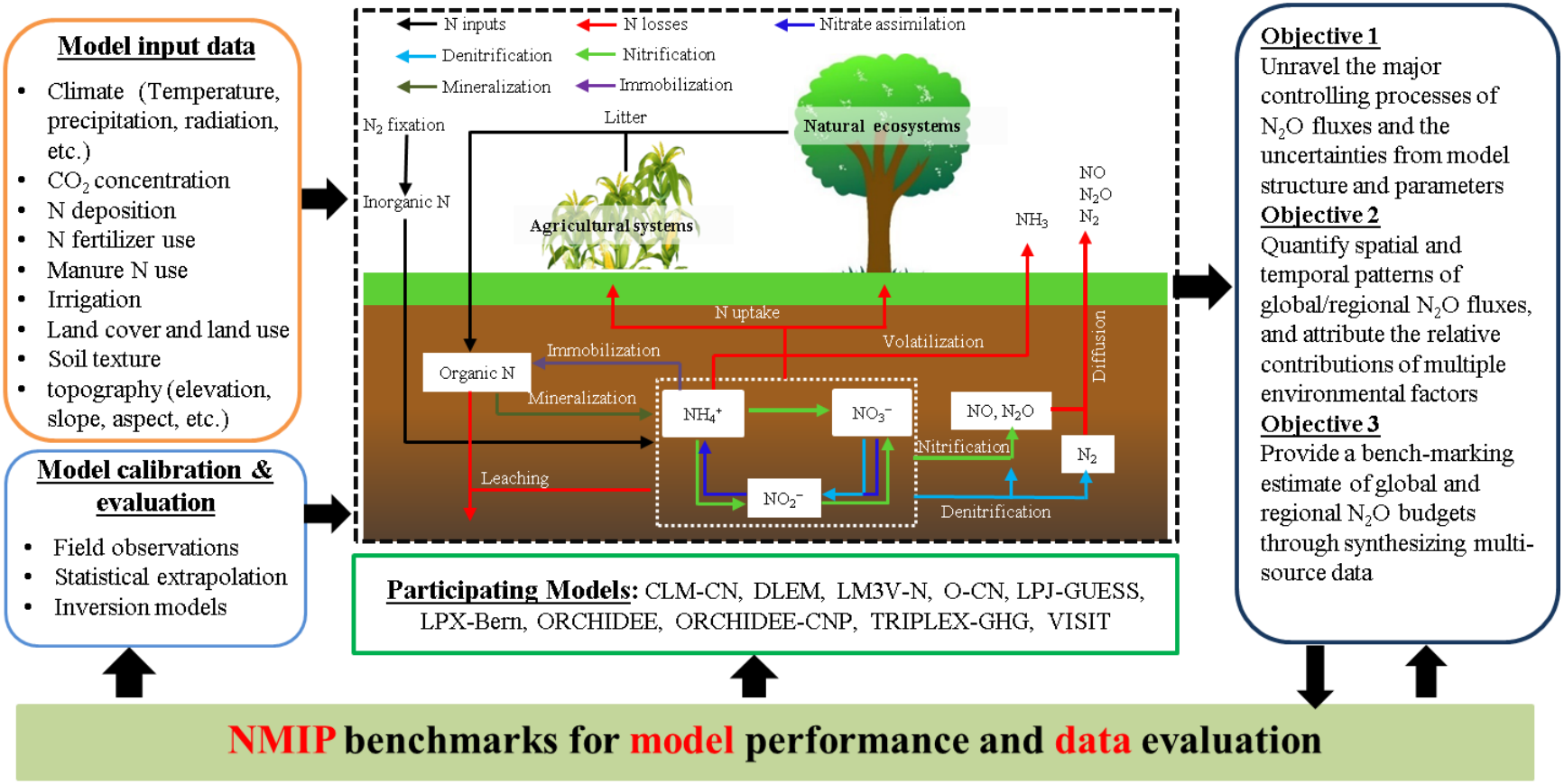

Figure 1. The framework of the N_2O Model Intercomparison project (NMIP)

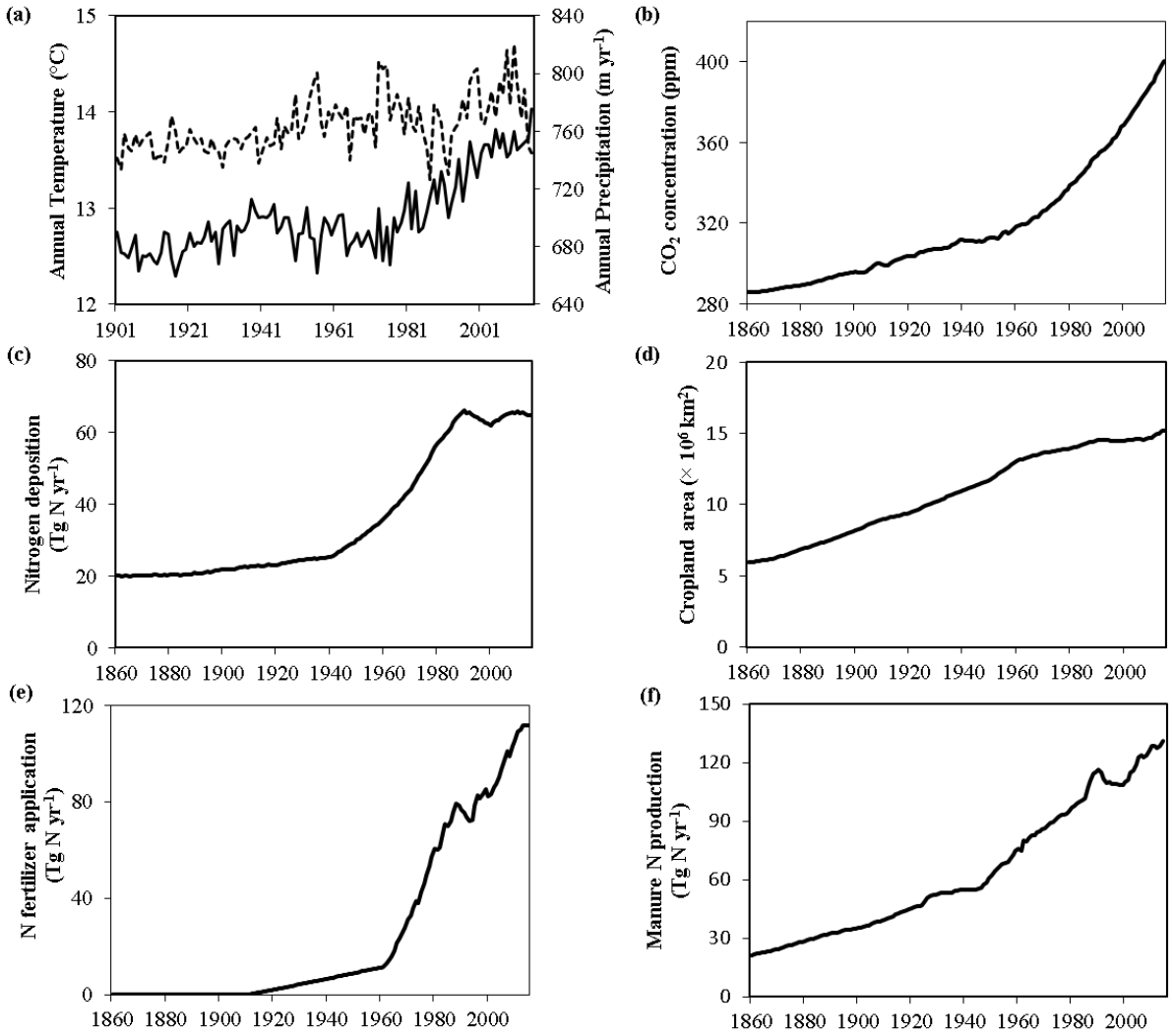

Figure 2. Evolution of the major driving factors at the global level during 1901-2016. (a) Annual temperature (°C, solid line) and annual precipitation (mm, dash line), (b) atmospheric CO_2 concentration (ppm), (c) cropland area (million km^2), (d) N deposition (Tg N yr^{-1}), (e) N fertilizer application (Tg N yr^{-1}) during 1900-2013, and (f) manure N production (Tg N yr^{-1}).

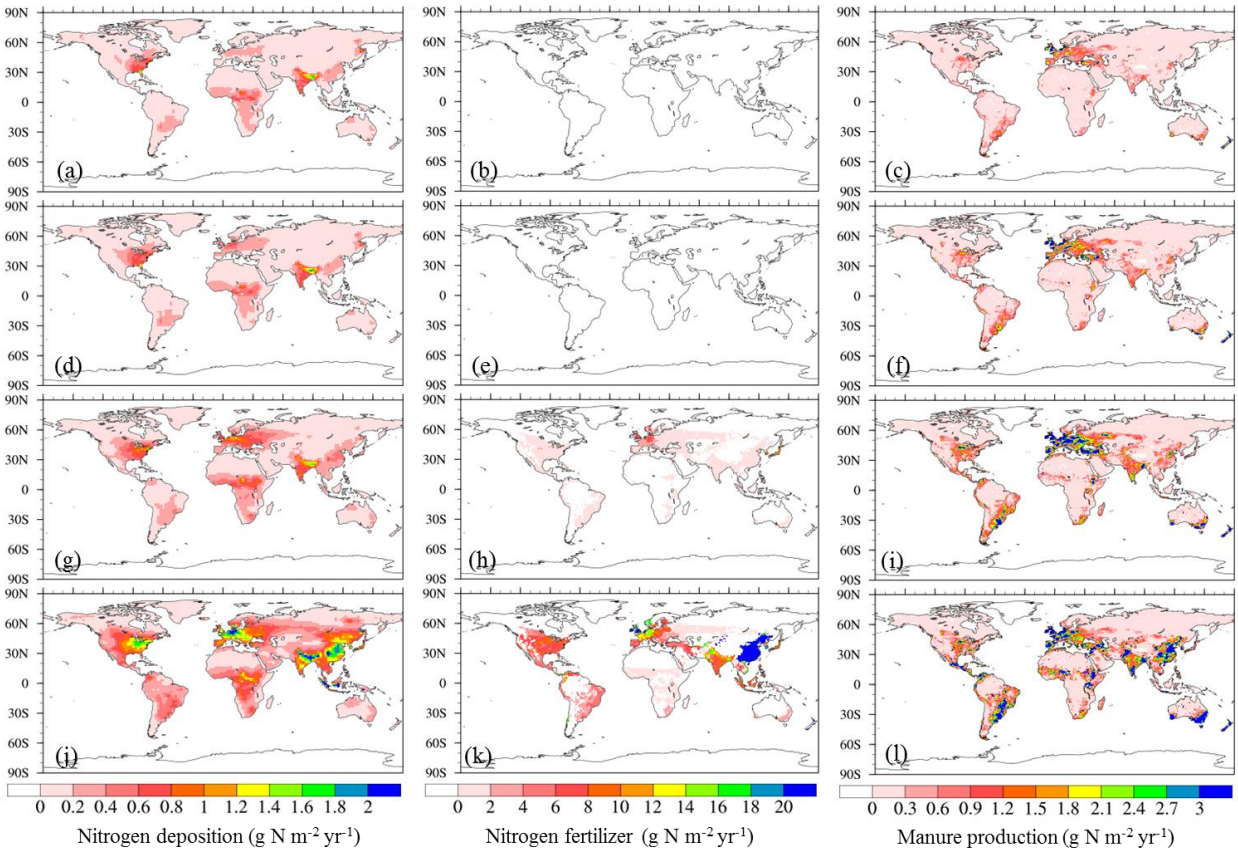

Figure 3. Spatial distribution of N deposition (a, d, g, j; g N m^{-2} yr^{-1}), N fertilizer application (b, e, h, k; g N m^{-2} cropland yr^{-1}), and manure N production (c, f, i, l; g N m^{-2} yr^{-1}) in 1860 (1st row), 1900 (2nd row), 1950 (3rd row), and 2015 (4th row).

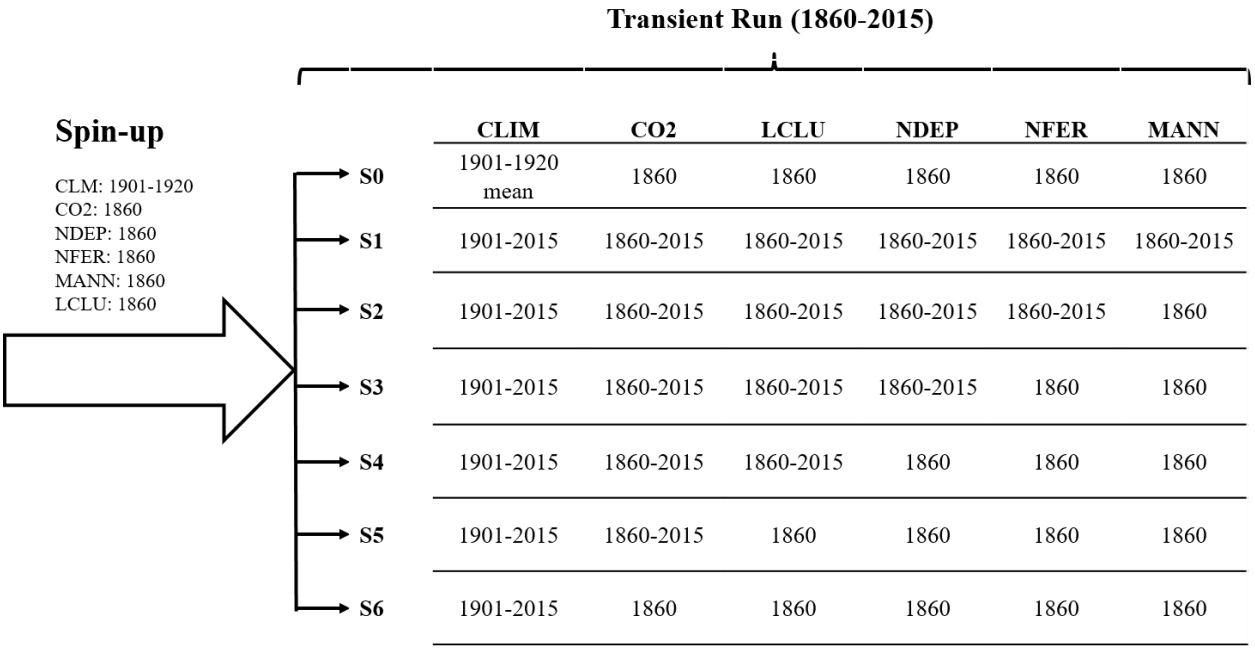

	CLIM	CO2	LCLU	NDEP	NFER	MANN
S0	1901-1920 mean	1860	1860	1860	1860	1860
S1	1901-2015	1860-2015	1860-2015	1860-2015	1860-2015	1860-2015
S2	1901-2015	1860-2015	1860-2015	1860-2015	1860-2015	1860
S3	1901-2015	1860-2015	1860-2015	1860-2015	1860	1860
S4	1901-2015	1860-2015	1860-2015	1860	1860	1860
S5	1901-2015	1860-2015	1860	1860	1860	1860
S6	1901-2015	1860	1860	1860	1860	1860

Figure 4. Model simulation experimental designs (Note: S0: reference (baseline); S1: CLIM+CO_2+LCLU+NDEP+NFER+MANN; S2: CLIM+ CO_2+LCLU+NDEP+NFER; S3: CLIM+ CO_2+LCLU+NDEP; S4: CLIM+ CO_2+LCLU; S5: CLIM+ CO_2; S6: CLIM). CLIM: climate, CO_2: atmospheric CO_2, LCLU: land cover and land use change, NDEP: N deposition, NFER: N fertilizer use, and MANN: manure N use

1021

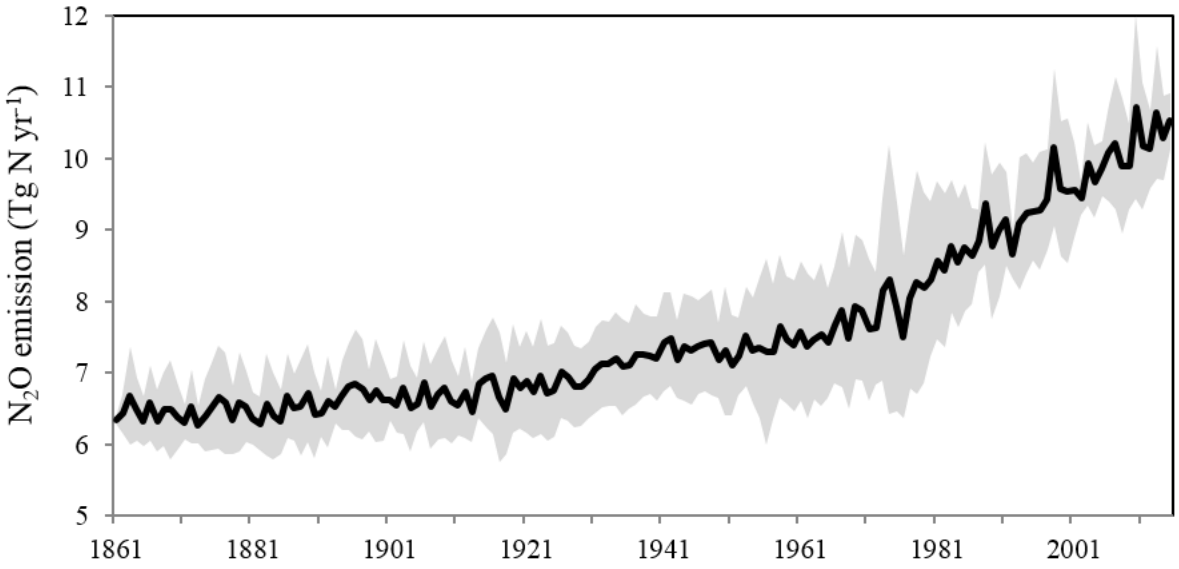

1022

1023 **Figure 5.** Interannual variations in N_2O emissions from global terrestrial ecosystems during
1024 1861-2015 as estimated by the average of three process-based models (DLEM, O-CN, and
1025 VISIT). The gray shades denote ± 1 standard deviation.
1026
1027

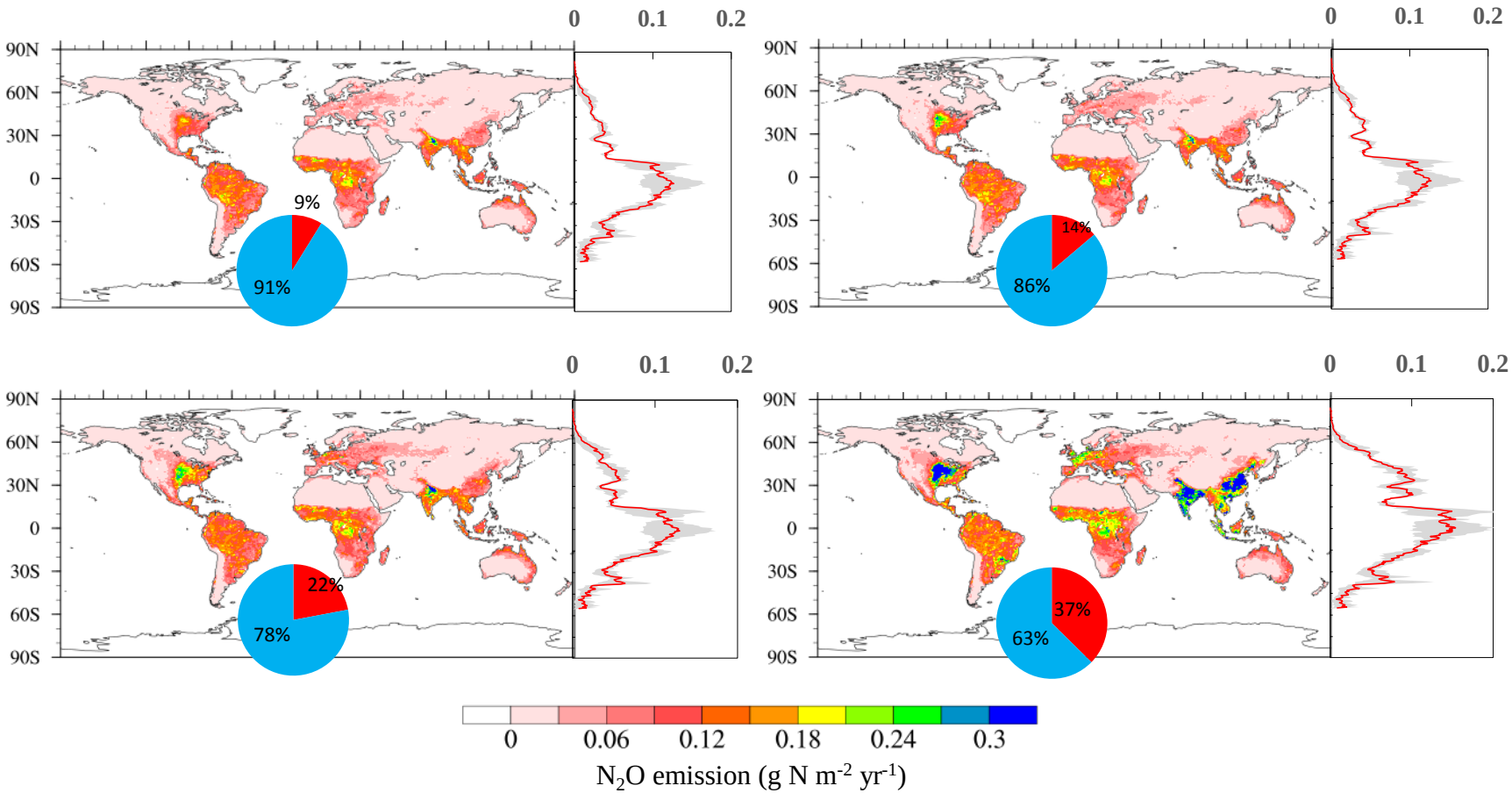

Figure 6. Spatial patterns and the latitudinal variations of mean annual N_2O emissions as represented by the mean estimates from DLEM, VISIT, and O-CN models in the (a) 1860s, (b) 1900s, (c) 1950s, and (d) 2001-2015. The pie charts indicate the relative contributions of natural vegetation (blue) and cropland (red) to the total N_2O emissions. The gray shades denote ± 1 standard deviation.

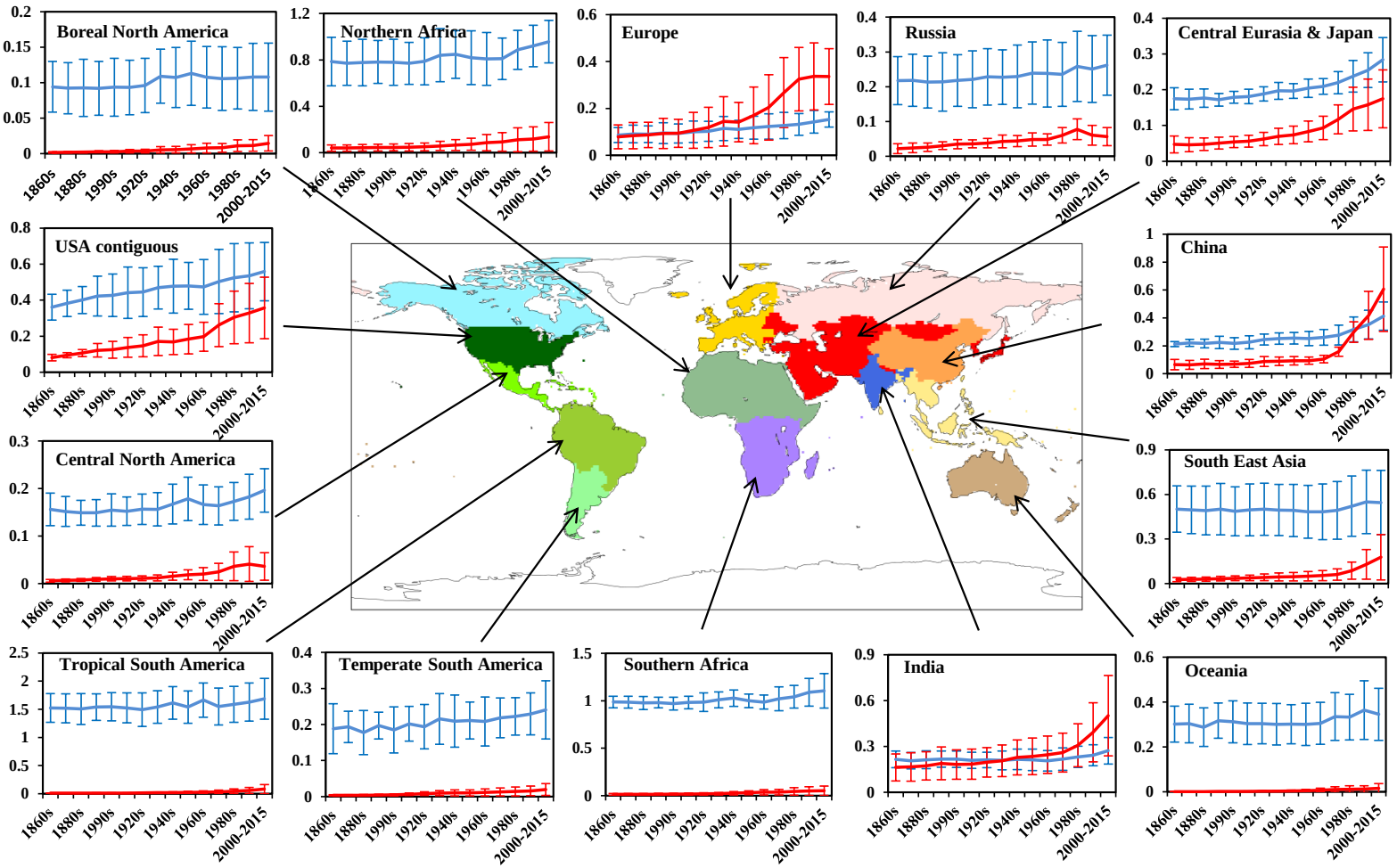

Figure 7. Decadal N_2O emissions (Tg N yr^{-1}) from the natural ecosystems (blue lines) and cropland (red lines) in 14 regions (region delineation is from the Global Carbon Project global CH_4 budget synthesis, Saunois et al., 2016). N_2O emissions are represented by the average of DLEM, VISIT, and O-CN model simulations. The error bars denote ± 1 standard deviation.